J. Fluid Mech. (1982), *vol.* 124, *pp.* 495–528
Printed in Great Britain

Sedimentation in a dilute polydisperse system of interacting spheres. Part 2. Numerical results

By G. K. BATCHELOR AND C.-S. WEN†
Department of Applied Mathematics and Theoretical Physics, University of Cambridge

(Received 21 January 1982)
Corrigendum Vol 137 pp 467-469

Analytical formulae for the effect of interaction between pairs of rigid spherical particles on the mean velocity of each species in a statistically homogeneous dilute polydisperse system were given in Part 1 (Batchelor 1982), and are here evaluated numerically. We have calculated the pair-distribution function and the associated value of the sedimentation coefficient for a wide variety of conditions of the two interacting species, including different values of the ratio of the radii of the spheres (λ), different values of the ratio of their (reduced) densities (γ), small and large values of the Péclet number of the interaction, and different forms of the potential of the mutual force exerted directly between the two spheres. Values of λ and γ such that some of the trajectories of one sphere centre moving under gravity alone relative to another are of finite length lie outside the scope of the calculations at large Péclet number, and the change of behaviour across the boundary of this excluded set of values leads to a complicated dependence of the sedimentation coefficient on λ and γ. At small Péclet number the behaviour is simpler, and a formula which represents the calculated values of the sedimentation coefficient over the whole range of values of λ and γ (on which the dependence is known to be linear) with fair accuracy in the absence of interparticle forces is devised. Our calculations of the effect of an interparticle force were based on the assumption of a high Coulomb barrier at a certain sphere separation which could be varied, and a van der Waals attractive force at larger separations. It appears that the direct contribution to the sedimentation coefficient made by gravity is always appreciably larger than that made either by relative Brownian diffusion of the two interacting spheres or by the interparticle force. However, all three of these (effective) forces normally have a significant influence on the pair-distribution function and thereby also affect the sedimentation coefficient indirectly. Some published observations of the mean particle velocity in monodisperse systems are interpreted in the light of the present calculations of the effect of interparticle forces.

1. Introduction

In this paper we describe numerical computations of the sedimentation coefficients for a dilute homogeneous polydisperse system using the formulae found in Part 1 (Batchelor 1982). The relevant formulae will be quoted from Part 1 without explanation of their origin, in exactly the same notation. It is hoped nevertheless that this present paper can be read independently by those who are interested primarily in the numerical results and their application. Our purpose is essentially practical,

† Present address: Anhui Institute of Optics and Fine Mechanics, P.O. Box 25, Hefei, Anhui, China.

viz. to provide calculated values of the fall speeds of the different types of particle which will allow the interpretation and extension of experimental data on hydrosol or aerosol dispersions.

The specific objective of the calculations is to obtain values of the sedimentation coefficient S_{ij} defined by the expression

$$\langle \mathbf{U}_i \rangle = \mathbf{U}_i^{(0)}\left(1 + \sum_{j=1}^{m} S_{ij}\phi_j\right) \quad (i = 1, 2, \ldots m) \tag{1.1}$$

for the mean velocity of rigid spheres of species i correct to the order of the first power of the total particle volume fraction ϕ ($= \Sigma_{j=1}^{m} \phi_j$). Here $\mathbf{U}_i^{(0)}$ is the velocity of an isolated sphere of species i moving under gravity and is a measure of one of the external forces on the system. The summation is over the m different species of particle in the system.

The sedimentation coefficient is a function of the ratios of the radii and of the reduced densities of the spheres of species i and j denoted by

$$\lambda = \frac{a_j}{a_i}, \quad \gamma = \frac{\rho_j - \rho}{\rho_i - \rho},$$

where ρ is the density of the fluid, and of the two dimensionless parameters measuring the relative magnitudes of the different kinds of force acting on the spheres. One is the Péclet number

$$\mathscr{P}_{ij} = \frac{\frac{1}{2}(a_i + a_j)\, V_{ij}^{(0)}}{D_{ij}^{(0)}}, \tag{1.2}$$

which compares the relative motion of the spheres due to gravity ($\mathbf{V}_{ij}^{(0)}$ being defined as $\mathbf{U}_j^{(0)} - \mathbf{U}_i^{(0)}$, $= (\gamma\lambda^2 - 1)\,\mathbf{U}_i^{(0)}$) and that due to Brownian diffusion. Here $D_{ij}^{(0)}$ is the relative diffusivity of two spheres of species i and j which are far apart (and isolated from other spheres), that is,

$$D_{ij}^{(0)} = \frac{kT}{6\pi\eta}\left(\frac{1}{a_i} + \frac{1}{a_j}\right). \tag{1.3}$$

The other is $\Phi_{ij}^{(0)}/kT$, which compares the relative motion due to an interparticle force with potential $\Phi_{ij}(r)$, of which $\Phi_{ij}^{(0)}$ is a representative value, and that due to Brownian diffusion. The sedimentation coefficient depends on the statistical structure of the dispersion, which in this case of a dilute dispersion is represented by the pair-distribution function $p_{ij}(\mathbf{r})$, where $\mathbf{r}$ is the vector separation of the two sphere centres, but p_{ij} is fully determined by the above four dimensionless parameters.

The pair-distribution function $p_{ij}(\mathbf{r})$ satisfies a differential equation of Fokker–Planck type (equation (4.2) of Part 1), and when p_{ij} is known the sedimentation coefficient S_{ij} can be calculated from the expressions (6.2), (6.3) and (6.4) in Part 1 giving the direct contributions to S_{ij} due to gravity (with hydrodynamic interaction), interparticle forces, and relative diffusion respectively. We have calculated $p_{ij}(\mathbf{r})$ and S_{ij} for both very large and very small values of the Péclet number and for several different values of λ and γ in the absence of an interparticle force. The effect on the sedimentation coefficient of an interparticle force which incorporates both van der Waals attraction and electrostatic repulsion in a simplified way is also calculated for the case of equal-sized spheres at small Péclet number. In Part 1 there was given some analytical results for the asymptotic behaviour of S_{ij} as $\lambda \to 0$, $\lambda \to \infty$ or $|\gamma| \to \infty$ which are independent of Péclet number, and these will be compared with the numerical results.

The starting-point for our calculations of p_{ij} and S_{ij} is the set of numerical values

for the two-sphere mobility functions A_{11}, A_{12}, A_{22}, B_{11}, B_{12}, B_{22} (all functions of λ and s, $= 2r/(a_1+a_2)$) provided by the recent work of D. J. Jeffrey, who has kindly put his results at our disposal in advance of their publication (Jeffrey 1983). For general values of λ and s Jeffrey gives the coefficients in a double series of positive powers of λ and negative powers of s for each of these functions which may be summed by a computer. For small values of $s-2$ $(= \xi)$ the series become too slowly convergent to be useful, and Jeffrey gives supplementary formulae, obtained from near-field asymptotic analysis, of the type

$$A_{\alpha\beta} = C'_{\alpha\beta,1} + \xi C'_{\alpha\beta,2} + \xi^2 \log \xi C'_{\alpha\beta,3} + \xi^2 C'_{\alpha\beta,4}, \tag{1.4}$$

$$B_{\alpha\beta} = \frac{C''_{\alpha\beta,1} + C''_{\alpha\beta,2}(\log \xi^{-1})^{-1} + C''_{\alpha\beta,3}(\log \xi^{-1})^{-2}}{1 + C''_{\alpha\beta,4}(\log \xi^{-1})^{-1} + C''_{\alpha\beta,5}(\log \xi^{-1})^{-2}}, \tag{1.5}$$

in which $\alpha, \beta = 1, 2$ and the coefficients $C'_{\alpha\beta,1}, \ldots$ $C''_{\alpha\beta,1}, \ldots$ are known functions of λ. For some purposes we found that the simplified asymptotic forms

$$A_{\alpha\beta} = C'_{\alpha\beta,1} + \xi C'_{\alpha\beta,2}, \quad B_{\alpha\beta} = C''_{\alpha\beta,1} + \frac{C''_{\alpha\beta,2} - C''_{\alpha\beta,1} C''_{\alpha\beta,4}}{\log \xi^{-1}} \tag{1.6}$$

were sufficiently accurate.

2. Large values of the Péclet number (and $\Phi_{ij} = 0$)

When the effect of Brownian motion is neglected, and the effect of an interparticle force is ignored, the pair-distribution function is a function of r alone given by

$$\log p_{ij}(\mathbf{r}) = \int_s^\infty \left\{ \frac{2(L-M)}{sL} + \frac{1}{L}\frac{dL}{ds} \right\} ds \tag{2.1}$$

on any trajectory of one sphere centre relative to another which comes from and goes to 'infinity'. Here L and M are dimensionless functions of s defined by the expression

$$\mathbf{V}_{ij}(\mathbf{r}) = \mathbf{U}_j - \mathbf{U}_i = \mathbf{V}_{ij}^{(0)} \left\{ \frac{\mathbf{rr}}{r^2} L(s) + \left(\mathbf{I} - \frac{\mathbf{rr}}{r^2} \right) M(s) \right\} \tag{2.2}$$

for the relative velocity of the two sphere centres due to gravity. L and M are given in terms of λ, γ and the mobility functions A_{11}, A_{12}, A_{22}, B_{11}, B_{12}, B_{22} by the relations (2.17) and (2.18) in Part 1.

The only force acting on a particle in this case is gravity, and the sedimentation coefficient is given by

$$S_{ij}(\lambda, \gamma) = \int_2^\infty \left[\left(\frac{1+\lambda}{2\lambda} \right)^3 (A_{11} + 2B_{11} - 3) p_{ij} + \tfrac{1}{4}\gamma(1+\lambda)^2 \left\{ (A_{12} + 2B_{12}) p_{ij} - \frac{3}{s} \right\} \right] s^2 ds - \gamma(\lambda^2 + 3\lambda + 1). \tag{2.3}$$

Our calculations of S_{ij} are restricted to cases in which all the trajectories are open and extend to infinity and for which p_{ij} is consequently a function of r alone given by (2.1) over the whole field. We begin therefore by discussing the region of the (λ, γ)-plane to which our results apply.

2.1. *Values of λ and γ for which all trajectories are open*

The radial component of velocity of the centre of the j-sphere relative to that of the i-sphere is given by

$$\begin{aligned}\mathbf{r}\,.\,\mathbf{V}_{ij} &= \mathbf{r}\,.\,\mathbf{V}_{ij}^{(0)}\,L(s)\\ &= \mathbf{r}\,.\,\mathbf{U}_i^{(0)}\left\{\lambda^2\gamma A_{22}-A_{11}+\frac{2(1-\lambda^3\gamma)}{1+\lambda}A_{12}\right\}.\end{aligned} \tag{2.4}$$

This radial component is zero at all points on a sphere of radius R such that

$$\left\{\lambda^2\gamma A_{22}-A_{11}+\frac{2(1-\lambda^3\gamma)}{1+\lambda}A_{12}\right\}_{s=2R/(a_i+a_j)} = 0, \tag{2.5}$$

and it follows that trajectories in the region

$$a_i+a_j \leqslant r < R$$

cannot cross the sphere $r = R$ and so cannot extend to infinity. The question is: is this relation (2.5) satisfied for some value of R larger than a_i+a_j?

The answer to this question is provided by the work of Wacholder & Sather (1974). Using the numerical solution for the flow due to two spheres moving under the action of given forces obtained previously by Lin, Lee & Sather (1970), they calculated the relative trajectories of the two spheres for different values of λ and γ. They found that for each value of λ there is a range of values of γ for which the relation (2.5) is satisfied at some value of R and for which trajectories of finite length exist. The combinations of values of λ and γ for which some trajectories are of finite length and which are excluded from our calculations of the sedimentation coefficient are shown in figure 1 for $0 \leqslant \lambda \leqslant 1$; and for values of λ outside this range the excluded combinations may be deduced from the fact that the trajectories are unchanged when λ and γ are both replaced by their reciprocals.

It is useful, for the interpretation of our calculations of the pair-distribution function, to note the character of the family of trajectories at points in the various regions of figure 1. At points below the shaded region in figure 1 the j-sphere is lighter and smaller and everywhere moves upward relative to the i-sphere on trajectories which extend to infinity and which have forms like those shown in figure 2(*a*) for the case $\lambda = \frac{1}{2}$. At the lower boundary of the shaded region (at which $\gamma = \gamma_c$, say, γ_c being a function of λ), equation (2.5) is satisfied by $R = a_i+a_j$ (to a higher order than $R-(a_i+a_j)$). Then, as γ increases above γ_c, R increases and trajectories of finite length appear (see figure 2(*b*)). These finite trajectories have common end points, which are reached asymptotically and at which the two spheres are touching and have a vertical line of centres. At larger values of γ, not near to the lower bound of the range $\gamma_c < \gamma < \lambda^{-2}$, the finite trajectories change shape, and become closed curves which are traversed in a finite time (figure 2(*c*)). Then as $\gamma \uparrow \lambda^{-2}$, $R \to \infty$ and the relative velocity of two widely separated spheres tends to zero. Finally, when $\gamma > \lambda^{-2}$ the j-sphere has the larger fall speed in isolation and everywhere moves downward relative to the i-sphere on trajectories extending to infinity as sketched in figure 2(*d*).

Our calculations of the pair-distribution function and of the sedimentation coefficient are confined to values of λ and γ such that

$$0 < \lambda \leqslant 1, \quad -\infty < \gamma < \gamma_c \quad \text{or} \quad \gamma > \lambda^{-2} \tag{2.6}$$

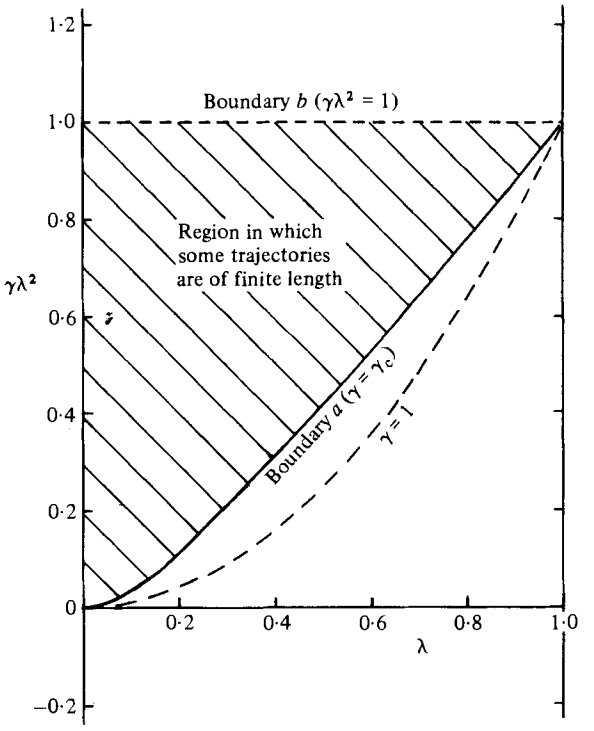

FIGURE 1. Values of λ and γ for which some members of the family of trajectories of one sphere centre relative to the other one are of finite length lie in the shaded region. The line $\gamma\lambda^2 = 1$ corresponds to two spheres having the same terminal velocity in isolation. In the case $\gamma = 1$ (two spheres of the same density), all the trajectories extend to infinity. (From Wacholder & Sather 1974.)

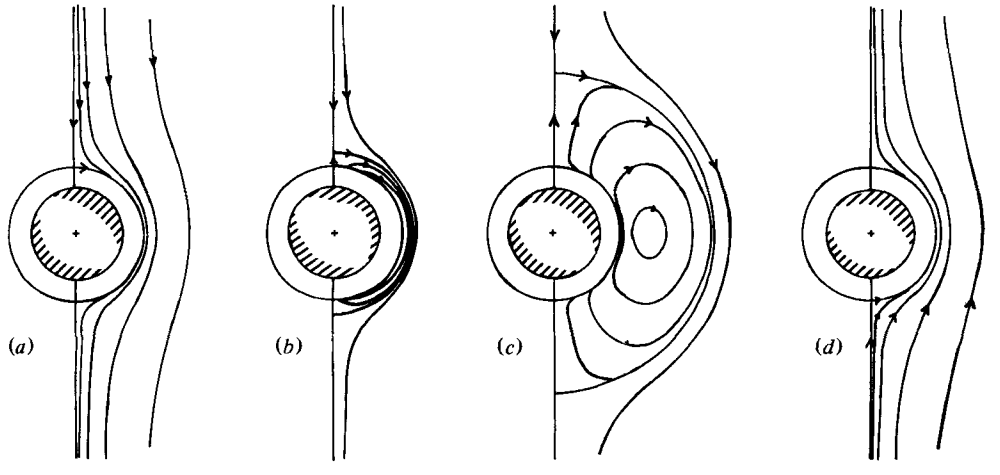

FIGURE 2. The family of trajectories of the centre of the j sphere relative to the centre of the i sphere, for $\lambda = \frac{1}{2}$; (*a*) $\gamma < \gamma_c$, (*b*) γ a little greater than γ_c, (*c*) γ significantly larger than γ_c but less than λ^{-2}, and (*d*) $\gamma > \lambda^{-2}$, where $\lambda = a_j/a_i$, $\gamma = (\rho_j - \rho)/(\rho_i - \rho)$. (From Wacholder & Sather 1974.)

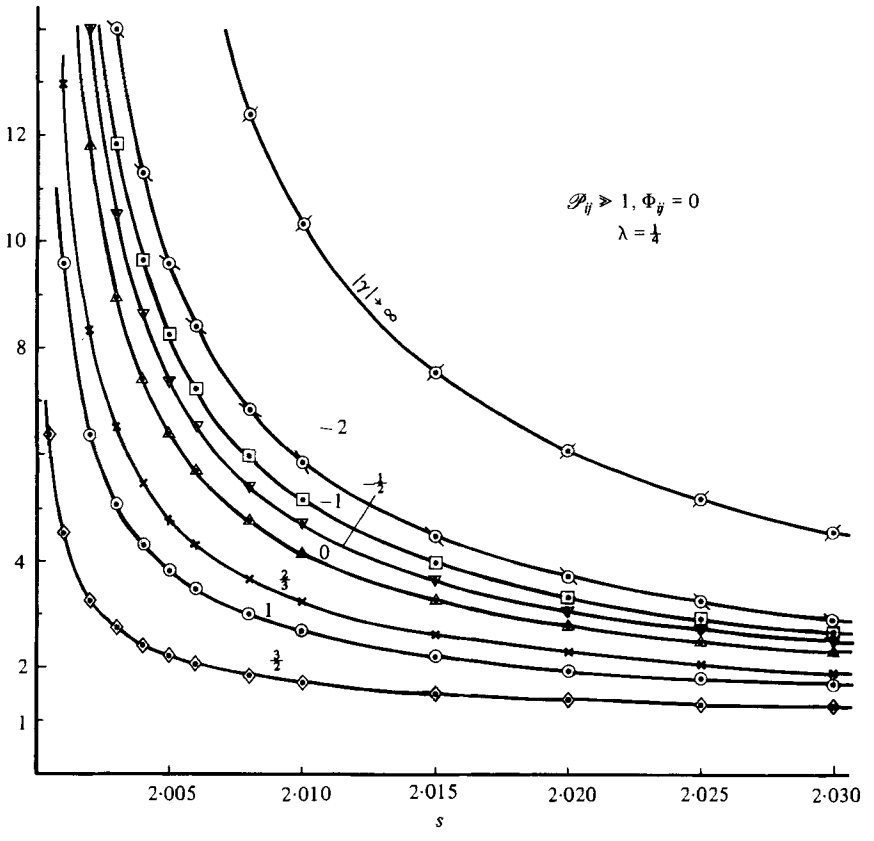

FIGURE 3. The pair-distribution function p_{ij} at large Péclet number for $\lambda = \frac{1}{4}$ and various values of γ. The abscissa is $s = 2r/(a_i + a_j)$. Note that p_{ij} is unchanged when λ and γ are replaced by λ^{-1} and γ^{-1}.

or, equivalently, if we define γ_c appropriately over the whole range of values of λ,

$$\lambda \geqslant 1, \quad -\infty < \gamma < \lambda^{-2} \quad \text{or} \quad \gamma > \gamma_c.$$

Since $\gamma_c > 1$ when $0 < \lambda < 1$ the important practical case of spheres of equal density is included in our calculations.

2.2. *The pair-distribution function*

In the 'far field', which we have chosen as $s > 5$, p_{ij} is given with sufficient numerical accuracy by the asymptotic form (4.15) in Part 1. For smaller values of s the integral in (2.1) was evaluated numerically over the range s to 5. The integrand was calculated from the series formulae for the mobility functions provided by Jeffrey for $2{\cdot}017 < s \leqslant 5$ and from the near-field asymptotic forms (1.4) and (1.5) for $2 < s \leqslant 2{\cdot}017$ (the dividing point $s = 2{\cdot}017$ being located where the two sources give approximately coincident results for the mobility functions).

For values of s very close to 2 the simplified asymptotic forms (1.6) are applicable, and the corresponding near-field asymptotic forms of the functions L and M are

$$L \sim L_1 \xi, \quad M \sim M_0 + M_1 (\log \xi^{-1})^{-1}, \tag{2.7}$$

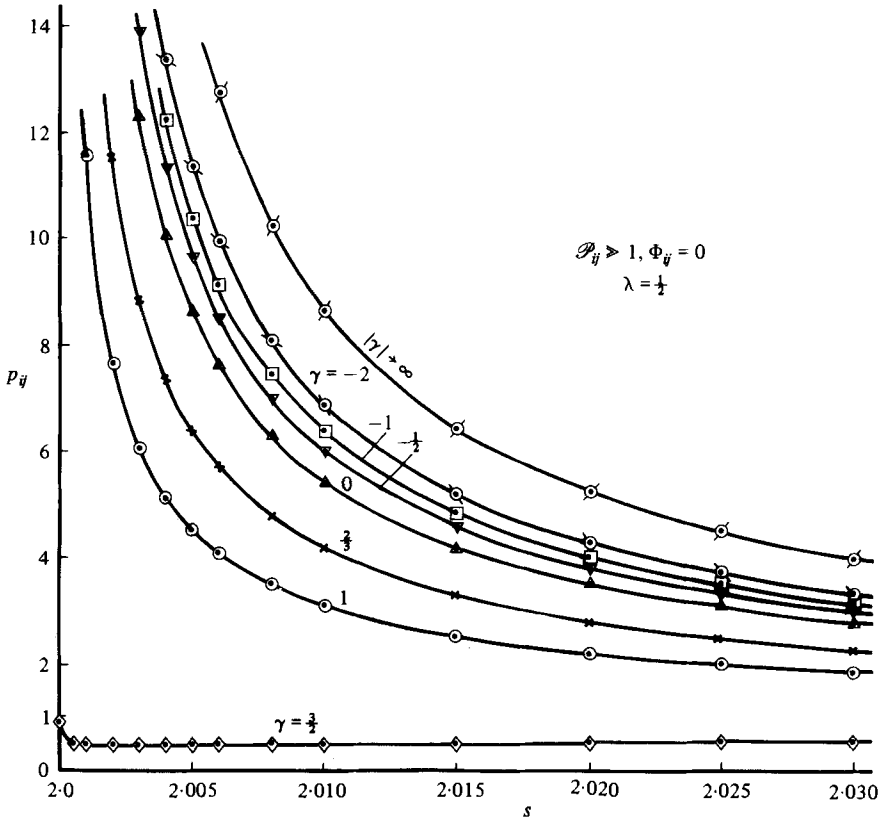

FIGURE 4. The pair-distribution function at large Péclet number for $\lambda = \frac{1}{2}$ and various values of γ.

where $\xi = s-2$ and L_0, M_0, M_1 are related to the coefficients $C'_{\alpha\beta,1}$, $C''_{\alpha\beta,1}$, etc in (1.6). The numerical convergence of the integral (2.1) as $s \downarrow 2$ was improved by first subtracting from the integrand the integrable function

$$\frac{x}{\xi} + \frac{y}{\xi \log \xi^{-1}}, \quad \text{where} \quad x = \frac{L_1 - M_0}{L_1}, \quad y = \frac{M_1}{L_1}; \tag{2.8}$$

the integrand is still singular at $s = 2$ but only weakly so. The asymptotic form of p_{ij}, as $s \downarrow 2$, is

$$p_{ij}(\mathbf{r}) \sim \frac{q_0}{\xi^x (\log \xi^{-1})^y}, \tag{2.9}$$

where the constant q_0 is not determinable from asymptotic analysis. We found that our calculated values of p_{ij} behaved like (2.9) in the range $2 < s < 2{\cdot}003$, and we therefore determined q_0 by making the expression (2.9) equal to the calculated value of p_{ij} at $s = 2{\cdot}001$. This gives a near-field asymptotic expression for p_{ij} which is useful for evaluation of the integral in (2.3).

Values of p_{ij} over the whole range $2 < s < \infty$ were calculated for all combinations of the values $\lambda = \frac{1}{4}, \frac{1}{2}, 1$ and $\gamma = -2, -1, -\frac{1}{2}, 0, \frac{2}{3}, 1, \frac{3}{2}, |\gamma| \to \infty$, and also for a few other isolated combinations. Figure 3 shows p_{ij} as a function of s for $\lambda = \frac{1}{4}$ and various values of γ, and figure 4 likewise for $\lambda = \frac{1}{2}$. The pair-distribution function is

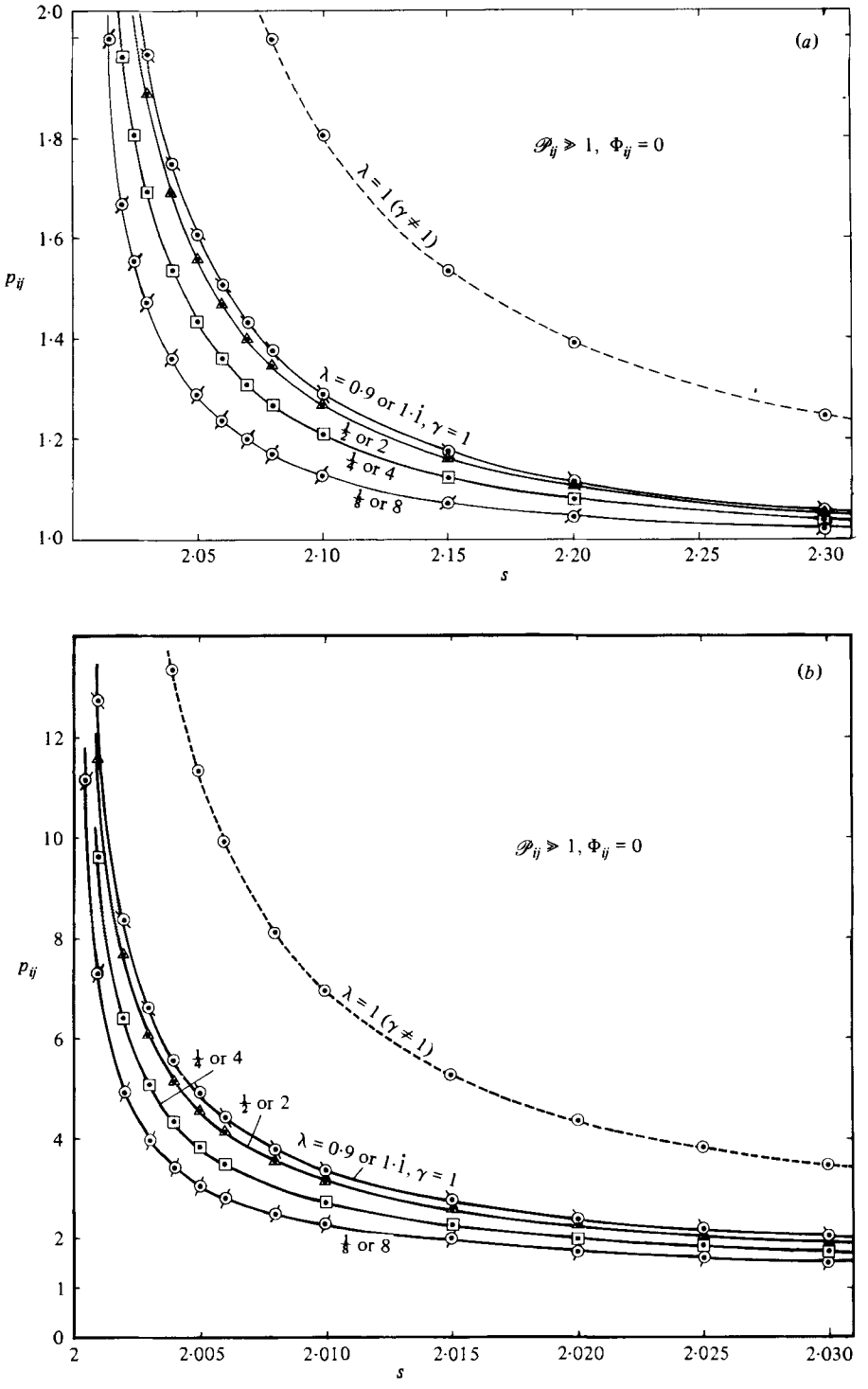

FIGURE 5. The pair-distribution function at large Péclet number for $\gamma = 1$ and various values of λ. The limit to which this family of curves is tending as $\lambda \to 1$ is different from the pair-distribution function calculated for $\lambda = 1$ and γ arbitrary (but $\neq 1$), this latter function being shown as a broken curve. In (*b*) the scales are enlarged to show the behaviour near $s = 2$.

unchanged when λ and γ are replaced by λ^{-1} and γ^{-1}, and figures 3 and 4 can also be interpreted as giving p_{ij} for $\lambda = 4$ and $\lambda = 2$ and the same (but rearranged) set of values of γ.

The untypical negative values of $p_{ij}-1$ for $\lambda = \frac{1}{2}$, $\gamma = \frac{3}{2}$ are associated with the proximity of the point representing this combination of values to the lower boundary of the shaded region in figure 1. As this boundary is approached from below, the function $L(s)$ (which measures the radial component of the relative velocity of the two spheres) and its derivative dL/ds become small for values of s near $s = 2$ and in consequence the sign of the integrand of (2.1) (measuring $\nabla . \mathbf{V}_{ij}/\mathbf{r} . \mathbf{V}_{ij}$) changes from positive to negative and its magnitude becomes large, leading to a change of sign of the integral. In terms of the asymptotic form (2.9), x decreases as the lower boundary of the shaded region in figure 1 is approached from below and passes through zero, becoming negative before the boundary is reached.

It was shown in Part 1 that, when λ is put equal to one, L and M, and hence also p_{ij}, are independent of γ. Figure 5 shows the calculated values of p_{ij} for this case. It was also pointed out in Part 1 that the value of p_{ij} at $\lambda = 1$, $\gamma = 1$ is not unique and depends on the way in which that point in the (λ,γ)-plane is approached. Figure 5 shows p_{ij} as a function of s as found from numerical integration for the cases $\gamma = 1$, $\lambda = \frac{1}{8}, \frac{1}{4}, \frac{1}{2}$ and 0·9. These four curves apply equally to the cases $\gamma = 1$, $\lambda = 8, 4, 2$ and 1·1 respectively, and it is evident from the trend of the curves that the curve corresponding to $\gamma = 1$, $\lambda \to 1$ must be close to that for $\gamma = 1$, $\lambda = 0{\cdot}9$ – and hence quite different from that for $\lambda = 1$ with γ arbitrary. It should be remembered that when $\lambda = 1$, $\gamma = 1$ the relative velocity of the two spheres is zero and so the Péclet number is then zero regardless of the value of the Brownian diffusivity; the above solutions of the approximate high-Péclet-number form of the equation for p_{ij} will thus be inapplicable in a neighbourhood of the point $\lambda = 1$, $\gamma = 1$ whose dimensions will depend on the values of $\frac{1}{2}(a_i + a_j)$ and $D_{ij}^{(0)}$.

2.3. *The values of* S_{ij}

For the evaluation of the integral in the expression (2.3) for S_{ij} we divided the range of integration into three parts. In the far field $5 \leqslant s < \infty$, p_{ij} and the mobility functions A_{11}, A_{12}, B_{11}, B_{12} can be replaced with sufficient accuracy by the series in powers of s^{-1} given in Part 1 and the integration can be made analytically. In the middle field defined by $2+\xi_1 \leqslant s \leqslant 5$, where ξ_1 is a small number to be specified later, the integral was evaluated numerically using the values of p_{ij} calculated as above and the values of the mobility functions as given by Jeffrey's series formula when $s \geqslant 2{\cdot}017$ and as given by his near-field asymptotic forms (1.4) and (1.5) at smaller values of s. In the near field $2 \leqslant s \leqslant 2+\xi_1$, we substituted the asymptotic form (2.9) for p_{ij} and the simplified asymptotic forms (1.6) for the mobility functions, whence the integrand becomes a sum of a number of terms of the form

$$\xi^{-\mu}(\log \xi^{-1})^{-\nu} \quad (\mu < 1).$$

Then since we have

$$\int_0^{\xi_1} \xi^{-\mu}(\log \xi^{-1})^{-\nu} d\xi = (1-\mu)^{\nu-1}\left\{\Gamma(1-\nu) - \eta^{1-\nu} \sum_{n=0}^{\infty} \frac{(-\eta)^n}{(1-\nu+n)\, n!}\right\},$$

provided $\nu < 1$, where $\eta = (1-\mu)\log \xi_1^{-1}$ and Γ denotes the complete gamma function, and since

$$\int_0^{\xi_1} \xi^{-\mu}(\log \xi^{-1})^{-\nu} d\xi = (\nu-1)^{-1}\xi_1^{1-\mu}(\log \xi_1^{-1})^{-\nu+1} - \frac{1-\mu}{\nu-1}\int_0^{\xi_1} \xi^{-\mu}(\log \xi^{-1})^{-\nu+1} d\xi$$

λ \ γ	−2	−1	−0·5	0	0·6̇	1	1·5	2·25	$\lim_{\lvert\gamma\rvert\to\infty} \frac{S_{ij}}{\gamma}$
0·25	−1·96	−2·00	−2·20	−2·56	−3·31	−3·83	−4·73	−6·90	1·97
0·5	−2·51	−2·27	−2·28	−2·53	−3·41	−4·29	−6·77	—	1·03
1				$S_{ij} = -2{\cdot}52 - 0{\cdot}13\gamma$ $(\gamma \neq 1)$					
2	3·18	−0·34	−1·89	−2·44	−9·85	−9·81	−11·16	−13·71	−3·79
4	26·63	10·05	2·03	−2·66	−19·55	−24·32	−32·71	—	−16·78

TABLE 1. Calculated values of the sedimentation coefficient S_{ij} for $\mathscr{P}_{ij} \gg 1$, $\Phi_{ij} = 0$, and different values of $\lambda(= a_j/a_i)$ and $\gamma(= (\rho_j - \rho)/(\rho_i - \rho))$

λ	S_{ij}	$S_{ij} + 2{\cdot}5 + \gamma$	λ	S_{ij}	$S_{ij} + \lambda^2 + 3\lambda + 1$
0·9	−5·29	−1·79	1·1̇	−5·95	−0·38
0·5	−4·29	−0·79	2	−9·81	1·19
0·25	−3·83	−0·33	4	−24·32	4·68
0·125	−3·68	−0·18	8	−78·53	10·47

TABLE 2. Calculated values of S_{ij} for $\gamma = 1$, $\mathscr{P}_{ij} \gg 1$, $\Phi_{ij} = 0$, and different values of $\lambda(= a_j/a_i)$, compared with the theoretical asymptotic forms for $\lambda \to 0$ and $\lambda \to \infty$

for any value of ν (except $\nu = 1$), the value of the contribution to the integral (2.1) from the near-field range can be found accurately.

Our procedure for the determination of ξ_1 was to take several small values and calculate the corresponding contributions to the integral (2.1) from the middle and near fields in the above way for each of these trial values of ξ_1, and then to choose a value such that the sum of these two contributions is stationary in the neighbourhood of the chosen value. We found that usually there was very little variation in the sum of these two contributions as ξ_1 was varied over the range 0·001–0·004, and so our normal choice was $\xi_1 = 0{\cdot}003$.

The calculated values of S_{ij} for all those combinations of λ and γ for which the pair-distribution function had been calculated are given in tables 1 and 2. The values of S_{ij} given in these tables should be correct to the first decimal place.

As $|\gamma| \to \infty$, p_{ij} tends to a finite limit and so S_{ij} is a linear function of γ at large values of $|\gamma|$; the calculated value of the coefficient of γ in this linear relation is shown in the last line of table 1. When $\lambda = 1$, p_{ij} is independent of γ and so S_{ij} is a linear function of γ in this case also, viz.

$$(S_{ij})_{\lambda=1} = -2{\cdot}52 - 0{\cdot}13\gamma \quad (\gamma \neq 1). \tag{2.10}$$

Feuillebois (1980) has also made a numerical calculation of S_{ij} at large Péclet number for the case $\lambda = 1$, and finds $S_{ij} = -2{\cdot}7 + 0{\cdot}1\gamma$. The small numerical differences are possibly a consequence of Feuillebois using different (and less accurate) data for the mobility functions in the near field.

The variation of S_{ij} with γ for various given values of λ is shown graphically in figure 6, and with λ for given γ in figure 7. Some of the curves have two sections with quite different behaviours, separated by a gap corresponding to values of λ and γ which lie within the excluded shaded area of figure 1. The termination of a section at the lower boundary of the excluded region of figure 1 (or at the extension of this boundary to values of λ outside the range $0 \leqslant \lambda \leqslant 1$) is labelled a, and a termination

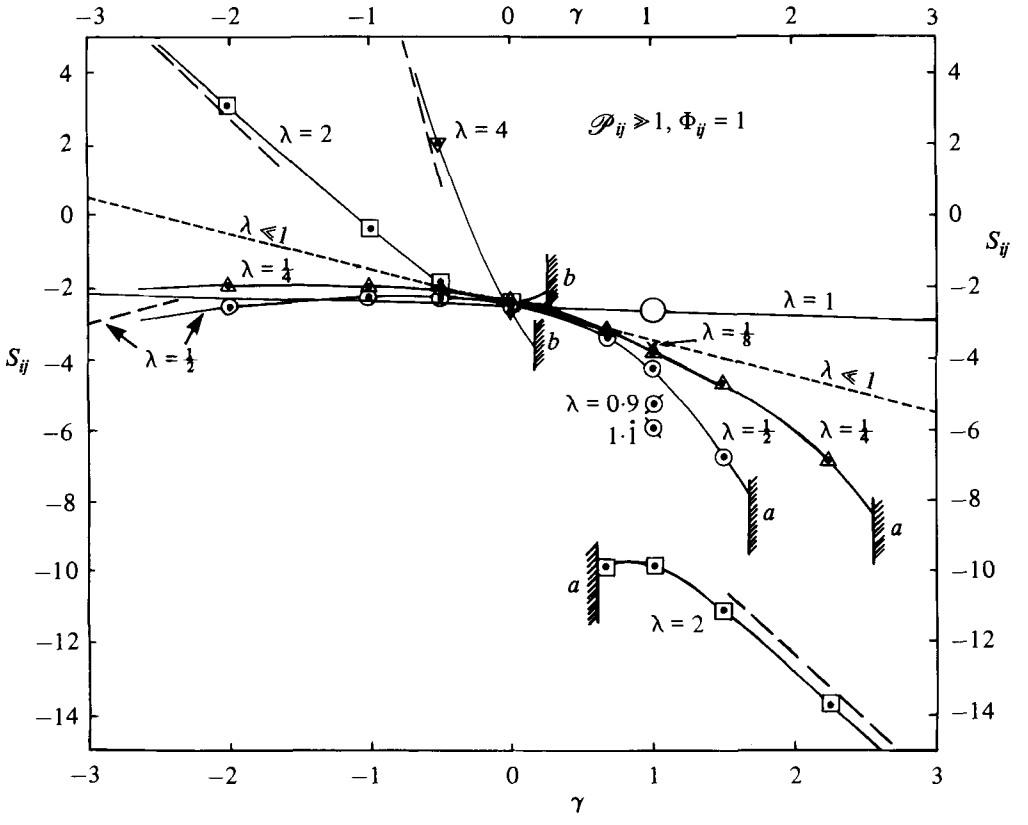

FIGURE 6. The sedimentation coefficient S_{ij} at large Péclet number as a function of γ for various values of λ. The shaded barriers indicate the lower (*a*) and upper (*b*) boundaries of the region of the (γ,λ)-plane in which some trajectories are of finite length (see figure 1).

at the upper boundary, where $\lambda^2\gamma = 1$, is labelled *b*. The large circle around the point corresponding to $\lambda = 1$, $\gamma = 1$ in each of figures 6 and 7 is a reminder (*a*) that the value at this point depends on how it is approached, and (*b*) that in a neighbourhood of this point the Péclet number is not large and the value of S_{ij} calculated as above is consequently not applicable. The calculated limiting value of S_{ij}/γ as $|\gamma| \to \infty$ for a given value of λ has been used to draw the broken lines in figure 6. Only the slopes of these broken lines are known, but the need for each of these lines to be an asymptote to the corresponding calculated curve both as $\gamma \to \infty$ and as $\gamma \to -\infty$ determines the positions of the lines quite closely.

It was shown in Part 1 that

$$S_{ij} \approx -2{\cdot}5-\gamma, \tag{2.11}$$

when $\lambda \ll 1$ at any value of the Péclet number. This linear relation in γ is shown as a dashed straight line in figure 6, and as a set of dashed asymptotes to the curves in figure 7 giving S_{ij} as a function of λ for given γ; in both figures (2.11) is clearly consistent with the calculated values of S_{ij}. Table 2 also shows a rapid approach of the values of S_{ij} to $-2{\cdot}5-\gamma$ as $\lambda \to 0$ in the particular case $\gamma = 1$. Another asymptotic result from Part 1 is that

$$S_{ij}+\gamma(\lambda^2+3\lambda+1) \to 0 \tag{2.12}$$

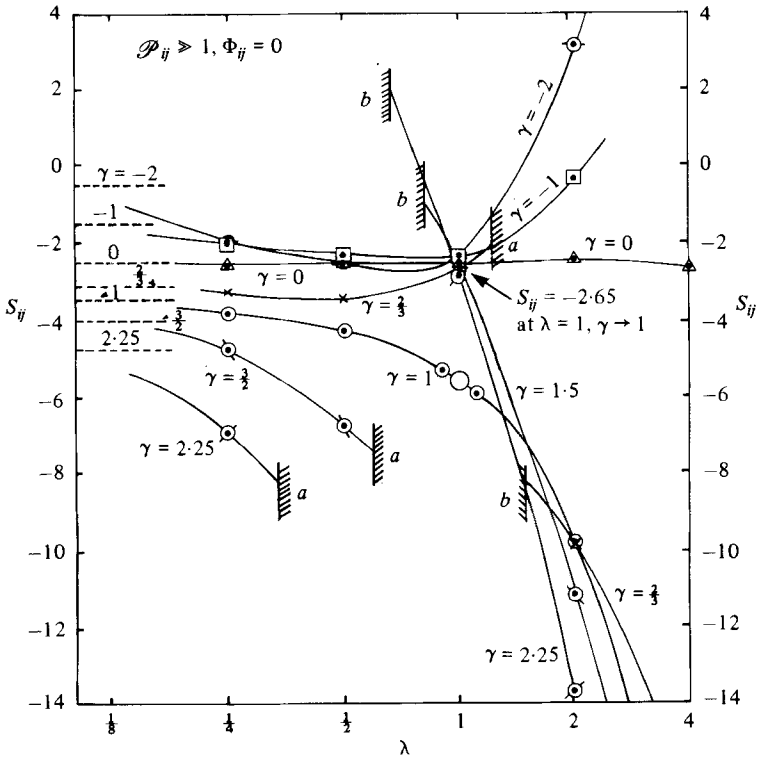

FIGURE 7. The sedimentation coefficient at large Péclet number as a function of λ for various values of γ.

as $\lambda \to \infty$ at any value of the Péclet number. This is not fully confirmed by the trend of the numerical results shown in the last column of table 2, and we believe it would be necessary to take the calculations to larger values of λ than 8 to reveal the approach to the asymptotic form. The relation (2.12) is a consequence of the deduction that $p_{ij} - 1$ is of order λ^{-3} when $\lambda \gg 1$, and it will be seen from figure 5 that the calculated values of $p_{ij} - 1$ for $\lambda = 2$, 4 and 8 have not begun to decrease, as λ increases, at the rate predicted analytically.

The bewildering pattern of variation of S_{ij} shown in figures 6 and 7 needs to be assimilated bit by bit. One striking feature of figure 6 is the quite small variation of S_{ij} with λ at $\gamma = 0$. This reflects the fact that when the j spheres are neutrally buoyant the main hydrodynamic effect of the presence of the j spheres is to cause more dissipation in the flow field generated by each falling i sphere. When $\lambda \ll 1$ this addition dissipation is given by the Einstein formula for the effective viscosity of a dispersion of spheres, and $S_{ij} \approx -2{\cdot}5$; and when λ is not small the hydrodynamic interaction of the i and j spheres modifies that value by an amount which is evidently small. The occurrence of positive values of S_{ij} is also worthy of note, since experience with monodisperse systems might suggest that 'hindered settling' is the norm in the absence of interparticle forces. The positive values of S_{ij} for $\gamma < 0$ and some values of λ greater than unity are no doubt a consequence of the strong counter flow associated with the rising j particles; and in the case $\lambda < 1$ the positive values of S_{ij} when $\gamma > \lambda^{-2}$ (see the last column of table 1) are a consequence of an i particle being carried downward when it is close to a faster-falling j particle.

3. Small values of the Péclet number (and $\Phi_{ij} = 0$)

The pair-distribution function in this case is not spherically symmetric and was found in Part 1 to be

$$p_{ij}(\mathbf{r}) = 1 + \frac{\mathbf{r} \cdot \mathbf{V}_{ij}^{(0)}}{r V_{ij}^{(0)}} \mathscr{P}_{ij} Q(s) \tag{3.1}$$

correct to the order of the first power of the Péclet number $\mathscr{P}_{ij}$, where $Q(s)$ satisfies the differential equation

$$\frac{d}{ds}\left(s^2 G \frac{dQ}{ds}\right) - 2HQ = s^2 W \tag{3.2}$$

subject to the boundary conditions

$$Q \to 0 \quad \text{as} \quad s \to \infty, \tag{3.3}$$

$$G\frac{dQ}{ds} = 0 \quad \text{at} \quad s = 2. \tag{3.4}$$

Here $G(s)$ and $H(s)$ determine the relative diffusivity of the two spheres in the directions parallel and perpendicular to the line of centres and are known multiples of the two-sphere mobility functions (see relations (2.19) and (2.21) of part 1), and

$$W(s) = \frac{2(L-M)}{s} + \frac{dL}{ds}.$$

The effect of gravity is here a perturbation of a system in equilibrium, and p_{ij} is consequently a linear function of γ, implying that

$$(\gamma\lambda^2 - 1)\, Q(s, \gamma, \lambda) = Q'(s, \lambda) + \gamma Q''(s, \lambda) \tag{3.5}$$

where Q' and Q'' are independent of γ and $Q' = -Q''$ when $\lambda = 1$. There is a corresponding decomposition of the sedimentation coefficient, viz.

$$S_{ij} = S'_{ij} + \gamma S''_{ij}. \tag{3.6}$$

It is useful moreover to identify the direct contributions made to S'_{ij} and S''_{ij} by gravity and by relative Brownian diffusion, to be labelled with the superscripts (G) and (B) respectively; thus

$$S'_{ij} = S'^{(G)}_{ij} + S'^{(B)}_{ij}, \quad S''_{ij} = S''^{(G)}_{ij} + S''^{(B)}_{ij}. \tag{3.7}$$

The analytical expressions for the coefficients $S'^{(G)}_{ij}$ and $S''^{(G)}_{ij}$ are seen from equation (6.10) in Part 1 to be

$$S'^{(G)}_{ij} = \left(\frac{1+\lambda}{2\lambda}\right)^3 \int_2^\infty (A_{11} + 2B_{11} - 3)\, s^2\, ds, \tag{3.8}$$

$$S''^{(G)}_{ij} = \left(\frac{1+\lambda}{2}\right)^2 \int_2^\infty \left(A_{12} + 2B_{12} - \frac{3}{s}\right) s^2 ds - (\lambda^2 + 3\lambda + 1). \tag{3.9}$$

Likewise from equation (6.12) in Part 1 we have

$$\begin{aligned} S^{(B)}_{ij} &= S'^{(B)}_{ij} + \gamma S''^{(B)}_{ij} \\ &= \left(\frac{1+\lambda}{2\lambda}\right)^2 \int_2^\infty \left\{\frac{A_{11} - B_{11}}{s} + \frac{1}{2}\frac{dA_{11}}{ds} - \frac{2(A_{12} - B_{12})}{(1+\lambda)s} - \frac{1}{1+\lambda}\frac{dA_{12}}{ds}\right\} (Q' + \gamma Q'')\, s^2\, ds. \end{aligned} \tag{3.10}$$

3.1. *Calculation of the pair-distribution function*

We solved the differential equation (3.2) for $Q(s)$ numerically, both for $\gamma = 0$ and $\gamma = 1$, for each of several different values of λ. From these solutions $Q'(s)$ and $Q''(s)$ may be found although there was no necessity to do that explicitly.

As $s \to \infty$, both G and H approach unity and W is of order s^{-5}, in general. Consequently Q may be written as

$$Q = \frac{\kappa}{s^2} + \sum_{n=3}^{\infty} \frac{Q_n}{s^n} \tag{3.11}$$

when $s \gg 1$, where κ is unknown and Q_n may be found in terms of κ by substituting (3.11) in the equation (3.2), writing G, H and W similarly as power series in s^{-1} with the aid of the asymptotic developments given in Part 1, and equating coefficients of s^{-n}. Our procedure for solving (3.2) was to guess a value of κ, thereby determining $Q(s)$ numerically in the 'far field' $s \geqslant 5$, and then to integrate the equation numerically from $s = 5$ to smaller values of s. The numerical values of G, H and W required for this integration were calculated from the series formulae for the mobility functions provided by Jeffrey (1982) for $2{\cdot}017 < s \leqslant 5$ and from Jeffrey's near-field asymptotic forms (1.4) and (1.5) for $2 < s \leqslant 2{\cdot}017$. The correctness of the assumed value of κ was judged by whether the inner boundary condition (3.4) was found to be satisfied; if it was not, further trials were needed.

In the neighbourhood of $\xi (= s-2) = 0$, the functions G, H and W have the behaviours

$$G \sim G_1 \xi, \quad H \sim H_0, \quad W \sim W_0,$$

where G_1, H_0 and W_0 are numbers dependent on λ (and on γ in the case of W_0) which can be found from the numerical coefficients in the simplified near-field asymptotic forms in (1.6). The differential equation (3.2) thus takes the approximate form

$$\xi \frac{d^2Q}{d\xi^2} + \frac{dQ}{d\xi} - \left(\frac{H_0}{2G_1}\right) Q = \frac{W_0}{G_1} \tag{3.12}$$

near $\xi = 0$. The general solution of (3.12) is

$$Q = -\frac{2W_0}{H_0} + \alpha I_0(\eta) + \beta K_0(\eta), \tag{3.13}$$

where $\eta = 2(H_0 \xi / 2G_1)^{\frac{1}{2}}$, α and β are constants to be determined, and I_0, K_0 are Bessel functions of imaginary argument. The inner boundary condition (3.4) is effectively

$$\lim_{\eta \to 0} \left(\eta \frac{dQ}{d\eta} \right) = 0,$$

and this requires $\beta = 0$ since $K_0(\eta)$ behaves as $\log \eta$ near $\eta = 0$. The solution correct to the order of ξ is thus

$$Q = -\frac{2W_0}{H_0} + \alpha(1 + \tfrac{1}{4}\eta^2),$$

which is equivalent to

$$2G_1 Q_0' - H_0 Q_0 = 2W_0, \tag{3.14}$$

where Q_0 and Q_0' are the values of Q and $dQ/d\xi$ at $\xi = 0$.

Our numerical integration of (3.2) with an assumed value of κ gave values of Q and $dQ/d\xi$ which varied very little in the range $0 < \xi \leqslant 0{\cdot}001$, and we equated Q_0 and Q_0' to the values found at $\xi = 0{\cdot}0005$. If two trial values of κ gave values of

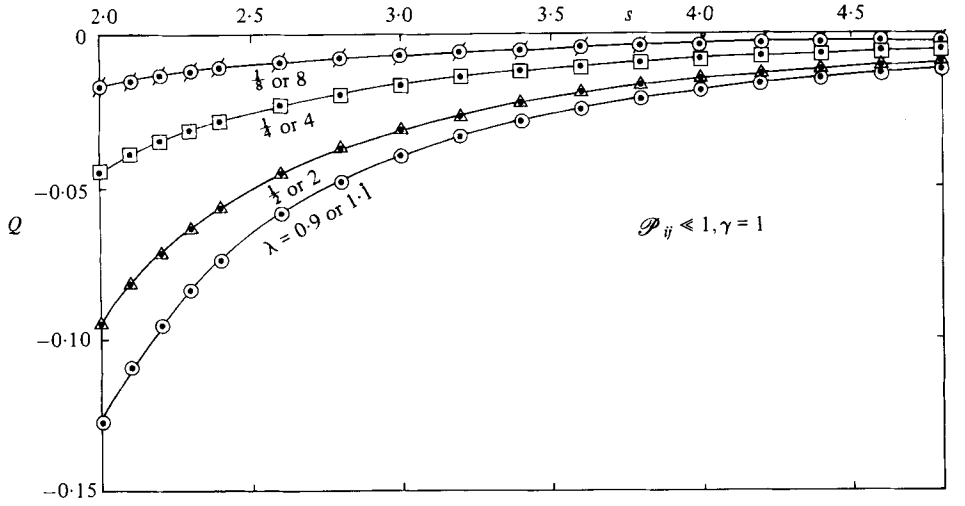

FIGURE 8. The perturbation of the pair-distribution function at small Péclet number (see (3.1)), for $\gamma = 1$ and various values of λ.

$2G_1 Q_0' - H_0 Q_0$ which both differed from $2W_0$, the computer sought the value of κ for which (3.14) was satisfied by successive interpolation.

As a check on the accuracy of our numerical solution, we calculated the value of

$$\int_2^\infty (2HQ + s^2 W)\, ds. \tag{3.15}$$

This integral is zero when Q satisfies equation (3.2), and when evaluated from our numerical solution for Q the integral was typically of magnitude about 0·01.

Our calculated values of Q as a function of s for $\gamma = 1$ and $\lambda = \frac{1}{8}, \frac{1}{4}, \frac{1}{2}$, 0·9 are shown in figure 8, and those for $\gamma = 0$ and $\lambda = \frac{1}{8}, \frac{1}{4}, \frac{1}{2}$, 1, 2, 4, 8 are shown (on a different scale) in figure 9. The function $Q(s)$ for any other value of γ can be obtained from these two sets of curves with the aid of (3.5). Again there is a difference between the pair-distribution function for $\lambda = 1$ with γ having any value except unity and the function for $\gamma = 1$ with λ tending to unity (reflecting the difference between the values of W in these two cases).

It will be noticed that, whereas the values of Q for given s and $\gamma = 1$ seem to be tending to zero as λ becomes large, those for $\gamma = 0$ are actually increasing as λ is changed from 1 to 2 to 4 and to 8, although according to the theoretical result in Part 1 $Q \to 0$ as $\lambda \to \infty$ for given s. In general, W and hence also Q are of order λ^{-3} when $\lambda \gg 1$, but $\gamma = 0$ is a special case owing to the occurrence of the products $\lambda^2\gamma$ and $\lambda^3\gamma$ in the expressions for L and M in (2.17) and (2.18) in Part 1, and W and hence also Q are of order λ^{-1} when $\lambda \gg 1$ in the case $\gamma = 0$. The convergence of Q to zero as $\lambda \to \infty$ is thus rather slow when $\gamma = 0$. The trend of the curves in figure 9 suggests that at larger values of λ than 8 the curves would begin to approach the axis $Q = 0$.

3.2. *The values of S'_{ij} and S''_{ij}*

We calculated the integrals in (3.8) and (3.9) using the data available for the mobility functions: far-field asymptotic forms (and analytical integration) for $5 \leqslant s < \infty$, the series formulae from Jeffrey (1983) for $2{\cdot}017 < s \leqslant 5$, and the near-field asymptotic

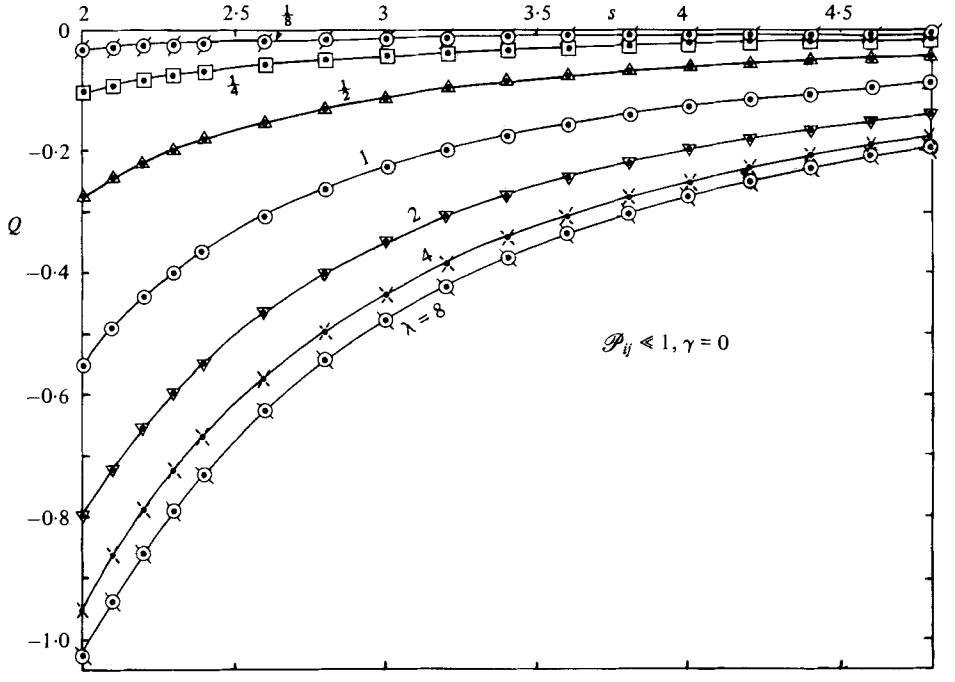

FIGURE 9. The perturbation of the pair-distribution function at small Péclet number, for $\gamma = 0$ and various values of λ. The same set of curves apply to $|\gamma| \to \infty$ when λ is replaced by λ^{-1}.

λ	$S'^{(G)}_{ij}$	$S'^{(B)}_{ij}$	S'_{ij}	$S''^{(G)}_{ij}+\lambda^2+3\lambda+1$	$S''^{(B)}_{ij}$	$S''_{ij}+\lambda^2$ $+3\lambda+1$	$(S_{ij})_{\gamma=1}+\lambda^2+3\lambda+1$
0·125	−2·34	0·03	−2·31	0·01	−0·01	0	−2·31
0·25	−2·24	0·07	−2·17	0·04	−0·04	0	−2·17
0·5	−2·09	0·15	−1·94	0·12	−0·12	0	−1·94
0·9	−1·88	0·25	−1·63	0·25	−0·24	0·01	−1·62
1·0	−1·83	0·27	−1·56	0·28	−0·27	0·01	−1·55
1·1	−1·78	0·28	−1·50	0·32	−0·30	0·02	−1·48
2	−1·45	0·35	−1·10	0·48	−0·47	0·01	−1·09
4	−1·04	0·41	−0·63	0·64	−0·68	−0·04	−0·67
8	−0·69	0·45	−0·24	0·75	−0·88	−0·13	−0·37

TABLE 3. Calculated values of the coefficients S'_{ij}, S''_{ij} (defined by the relation $S_{ij} = S'_{ij} + \gamma S''_{ij}$) for $\mathscr{P}_{ij} \ll 1$, $\Phi_{ij} = 0$, and different values of $\lambda (= a_j/a_i)$. The superscripts (G) and (B) denote the direct contributions made by gravity and Brownian diffusion.

forms (1.4) and (1.5) for $2 < s \leqslant 2{\cdot}017$. Likewise the integral in the expression (3.10) for $S^{(B)}_{ij}$ was calculated for $\gamma = 0$ and for $\gamma = 1$ using the previously calculated values of $Q(s)$ for those values of γ, whence $S'^{(B)}_{ij}$ and $S''^{(B)}_{ij}$ follow from

$$S'^{(B)}_{ij} = (S^{(B)}_{ij})_{\gamma=0}, \quad S''^{(B)}_{ij} = (S^{(B)}_{ij})_{\gamma=1} - (S^{(B)}_{ij})_{\gamma=0}. \tag{3.16}$$

In all cases the numerical integration could be carried down to $s = 2$ as the integrands are all finite there.

Table 3 shows the results of our calculations of $S'^{(G)}_{ij}$, $S'^{(B)}_{ij}$, $S''^{(G)}_{ij}$ and $S''^{(B)}_{ij}$ for $\lambda = \frac{1}{8}$,

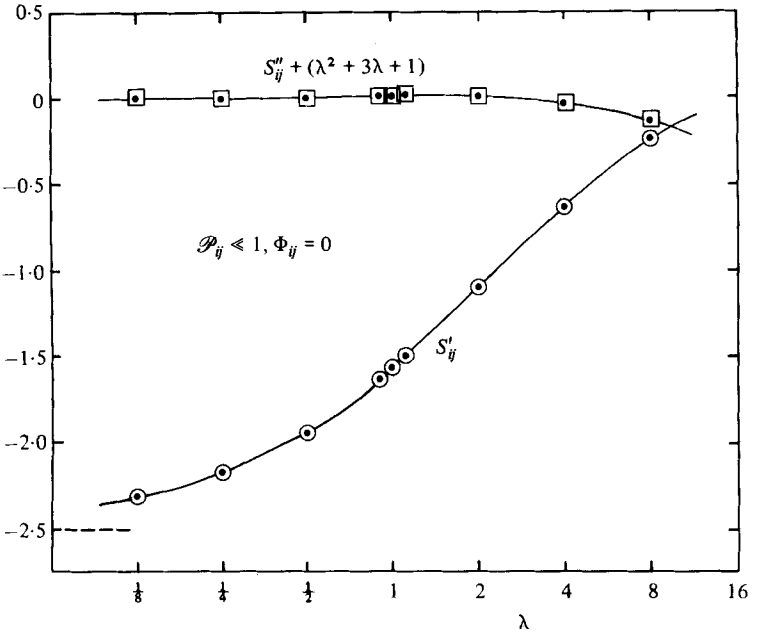

FIGURE 10. The sedimentation coefficients S'_{ij} and S''_{ij} (defined by $S_{ij} = S'_{ij} + \gamma S''_{ij}$) as functions of λ at small Péclet number. The coefficient S''_{ij} is plotted as $S''_{ij} + (\lambda^2 + 3\lambda + 1)$ to reduce the range of variation with λ.

$\frac{1}{4}$, $\frac{1}{2}$, 0·9, 1, 1·1, 2, 4, 8. In the case of $S''^{(G)}_{ij}$ we have subtracted $-(\lambda^2 + 3\lambda + 1)$ from the calculated values, since this is the known asymptotic form both for $\lambda \to 0$ (when only the term -1 is relevant) and for $\lambda \to \infty$ and the subtraction reduces greatly the variation of the tabulated numbers over the whole range. The approximate equality of magnitude of nearly all the adjoining numbers in the two columns headed $S''^{(G)}_{ij} + (\lambda^2 + 3\lambda + 1)$ and $S''^{(B)}_{ij}$ appears to be a coincidence of no significance, since these numbers come from integrals in (3.9) and (3.10) which have integrands of quite different analytical form. The sedimentation coefficient S_{ij} depends on γ (being equal to $S'_{ij} + \gamma S''_{ij}$), and values for the important particular case $\gamma = 1$ are shown in the last column of table 3, likewise after subtraction of the quantity $-(\lambda^2 + 3\lambda + 1)$ to reduce the tabulated variation. In the particular case $\lambda = 1$, $\gamma = 1$, when $S^{(B)}_{ij} = 0$, we recovered exactly the result $S_{ij} = -6{\cdot}55$ obtained by Batchelor (1972) for a monodisperse system; the integrals in (3.8) and (3.9) have integrands which are finite everywhere and the improved data on the mobility functions available to us has not led to any change of the earlier numerical result.

Figure 10 shows calculated values of S'_{ij} and $S''_{ij} + (\lambda^2 + 3\lambda + 1)$ as functions of λ (with a logarithmic scale for λ). It is evident that S'_{ij} approaches $-2{\cdot}5$ and that S''_{ij} approaches -1 as $\lambda \to 0$, in accordance with the asymptotic relations established (for any Péclet number) in Part 1. The theoretical predictions that $S'_{ij} \to 0$ and $S''_{ij} + (\lambda^2 + 3\lambda + 1) \to 0$ as $\lambda \to \infty$ are not in such clear agreement with the calculated values, but that is believed to be because the calculations have not been taken to a sufficiently large value of λ. The convergence of the sedimentation coefficients in table 3 to their asymptotic values as $\lambda \to \infty$ is slow and does not begin to be apparent until λ exceeds 8. We calculated the values of $S'^{(G)}_{ij}$ and $S''^{(G)}_{ij} + (\lambda^2 + 3\lambda + 1)$ (these being coefficients not requiring a calculation of the pair-distribution function) at

values of λ increasing by a factor 2 up to 1024, and found that they tended to $-12\lambda^{-1}$ and $70\lambda^{-1}$ respectively, with $S''^{(G)}_{ij}+(\lambda^2+3\lambda+1)$ having a maximum somewhere near $\lambda = 16$.

A striking feature of the calculated values shown in table 3 is the smallness of $|S'^{(B)}_{ij}|$ relative to $|S'^{(G)}_{ij}|$, except when $\lambda \gg 1$, and the (more marked) smallness of $|S''^{(B)}_{ij}|$ relative to $|S''^{(G)}_{ij}|$. At no value of λ is $|S''^{(B)}_{ij}|$ more than 5 percent of $|S''^{(G)}_{ij}|$. The approximate relation

$$S_{ij} \approx S'^{(G)}_{ij} + \gamma S''^{(G)}_{ij} \tag{3.17}$$

which ignores the direct contribution from Brownian motion (while retaining the indirect effect, which is to make the pair-distribution function nearly uniform) would be sufficiently accurate for many practical purposes, except for $\lambda \gg 1$ and values of γ near zero when the dominance of the second term in (3.17) is eliminated.

4. The effect of an interparticle force at small Péclet number

The numerical results reported in the two preceding sections and the analysis described in Part 1 together provide a general understanding and description of the effects of hydrodynamic interactions and of Brownian diffusion on sedimentation velocities in a dilute polydisperse system. There remains the effect of an interparticle force derived from the potential $\Phi_{ij}(r)$. The analysis in Part 1 was less complete in its consideration of effects of an interparticle force, and the same is true of our numerical calculations. This incompleteness is partly a consequence of the mathematical difficulty of investigating the motions of two nearly touching particles when all three of the relevant forces – gravity, effective diffusive force, interparticle force – are significant and many of the associated functions are singular; and partly it reflects the problems arising from the need to introduce additional independent parameters in a problem which already has too many for comfort.

4.1. *The assumed interparticle force potential*

The force exerted between two neighbouring colloidal particles in a stable dispersion is usually a resultant of the van der Waals attractive force and an electrostatic repulsive force between charges which are held at the surfaces of the two particles and screened by the presence of counter-ions in the double layers surrounding each particle. The dependence of the potential of the van der Waals force on the distance between two spheres is fairly well established, and a commonly used expression for the potential in the case of two spheres of the same radius a in a nearly-touching position is

$$\Phi_{vdW} = -\frac{A}{12\xi(1+11{\cdot}2\xi a\lambda_d^{-1})}, \tag{4.1}$$

where $\xi = (r-2a)/a$, A is the composite Hamaker constant which depends on the atomic composition of both the particles and the fluid medium, and λ_d is the 'dispersion' wavelength usually taken as $0{\cdot}100\ \mu$m. This expression is believed to be applicable when $\xi a < \lambda_d/\pi\ (= 0{\cdot}032\ \mu\text{m})$. And at larger separations, where retardation effects are stronger, but with the gap between the two spheres still small compared with a radius ($\xi \ll 1$), the potential is given approximately by

$$-\frac{10^{-3}A}{\xi}\left\{\frac{6{\cdot}50}{\xi a\lambda_d^{-1}} - \frac{0{\cdot}305}{(\xi a\lambda_d^{-1})^2} + \frac{0{\cdot}0057}{(\xi a\lambda_d^{-1})^3}\right\}. \tag{4.2}$$

These two expressions were put forward first by Schenkel & Kitchener (1960), and have been used by many later workers. The electrostatic force potential is less well

established, and it also varies widely with the nature of the dispersion. The two main controlling parameters are the charge density at the surface of a particle, or equivalently the electric potential at the surface, and the thickness of the double layer surrounding each particle. The potential of the Coulomb repulsion between the two spheres varies relatively slowly for sphere separations smaller than a double layer thickness and falls off exponentially when ξ exceeds this thickness. Roughly speaking, the surface electric potential determines the magnitude of the potential barrier to close approach of the two spheres and the double layer thickness determines the location of the barrier. Absolute sphere size (or a/λ_d, if one wishes to list only dimensionless parameters) appears in the expressions (4.1) and (4.2), so a minimum of three independent parameters are needed to represent the resultant interparticle force in a stable dispersion. These are additional to the three parameters γ, λ, $\mathscr{P}_{ij}$ already introduced to describe interactions between two different particles in a polydisperse system.

We propose in this paper to present only a few exploratory calculations for spheres of equal size which show the general nature and magnitude of the effect of interparticle forces on sedimentation velocities. With this modest objective in mind we have adopted the following simplified form of the Coulomb repulsion potential:

$$\Phi_{\text{Coul}} = \begin{cases} \Phi_0 (\gg kT) & \text{for} \quad 0 < \xi < \xi_0 \\ 0 & \text{for} \quad \xi \geqslant \xi_0, \end{cases} \tag{4.3}$$

where $\xi_0 a$ can be identified roughly with the double-layer thickness. The Coulomb barrier is being assumed here to be high enough to exclude any particle pairs with a spacing (surface to surface) smaller than $\xi_0 a$, and at larger spacings the Coulomb force is zero. For the potential of the van der Waals force the expression (4.1) will be assumed to hold over the whole range of (small) values of ξ, despite the fact that for some part of that range $\xi a > 0{\cdot}032\ \mu$m and (4.2) is more appropriate. (The numerical difference between (4.1) and (4.2) in the range $\xi a > 0{\cdot}032\ \mu$m is not large, as may be seen from the fact that (4.1) asymptotes to $-0{\cdot}0074A(\xi^2 a\lambda_d^{-1})^{-1}$ when $\xi a\lambda_d^{-1} \gg 1$ and (4.2) to $-0{\cdot}0065A(\xi^2 a\lambda_d^{-1})^{-1}$.) And since the magnitude of the van der Waals potentials falls off much more rapidly than (4.1) or (4.2) as soon as the gap between the spheres ceases to be small compared with the smaller of the two sphere radii, we have assumed that the potential jumps to zero at $\xi = 0{\cdot}2$; some modification of (4.1) at larger values of ξ is needed in any event because some of the integrals in the sedimentation analysis would otherwise be divergent.

The resultant interparticle force potential, which is sketched in figure 11, is thus specified now by two parameters, viz. ξ_0 and a/λ_d. This is not put forward as a realistic form of the potential, but it has the merit of allowing an examination of the effect of varying the important parameter ξ_0 representing the double layer thickness without too many numerical complications. For sphere separations in the range $0 < \xi < \xi_0$ the Coulomb repulsion is dominant and the pair-distribution function is zero, whereas for $\xi_0 < \xi < 0{\cdot}2$ the interparticle force is attractive and there are more sphere pairs than in the absence of interparticle forces. Varying ξ_0 from zero to 0·2 thus changes the balance between the effect on sedimentation velocities of an excess number of close pairs resulting from attractive forces and the effect of a deficiency of close pairs resulting from Coulomb repulsion over a wide range. The depth of the secondary minimum of Φ at $\xi = \xi_0$ has a strong effect on the maximum of the pair-distribution function and, with our simple model, is determined directly by ξ_0.

Numerical values of the van der Waals potential function (4.1) are shown in figure

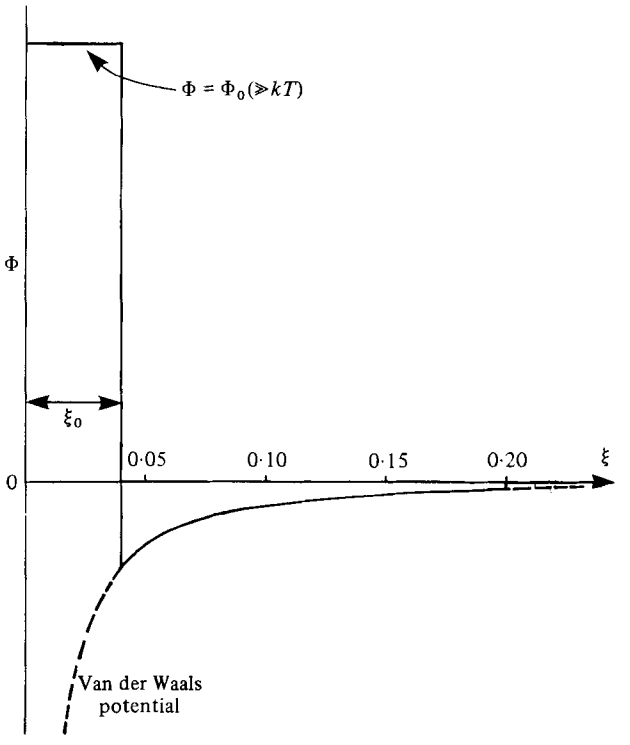

FIGURE 11. The simplified interparticle force potential (shown as a full curve) used in the calculations of sedimentation coefficients for equal sized spheres. Over the range $\xi_0 < \xi < 2{\cdot}2$ (where $\xi = (r-2a)/a$), Φ coincides with the van der Waals potential (4.1), and there is a high Coulomb barrier at $\xi = \xi_0$.

12 for four values of the radius of the two spheres, viz. $a = 0{\cdot}1, 0{\cdot}5, 1, 2$ μm, and with A having the value $5{\cdot}0 \times 10^{-21}$ J (i.e. $5{\cdot}0 \times 10^{-14}$ erg) appropriate to polystyrene latex particles in water, and $T = 290$ °K (so that $kT = 4{\cdot}0 \times 10^{-21}$ J and $A/kT = 1{\cdot}25$). These are the numerical values of Φ/kT to be used in calculations of the sedimentation coefficient for equal sized spheres at small Péclet number.

4.2. *Identical spheres*

This case of two spheres which have the same density as well as the same radius is relevant to a polydisperse system since self-interactions of one species affect the sedimentation velocity for that species, as well as being of considerable interest in its own right. The relative velocity of the two spheres due to gravity is zero here and the pair-distribution function has the form appropriate to 'structural equilibrium', viz. the Boltzmann distribution

$$p(\mathbf{r}) = \exp\{-\Phi(r)/kT\}. \tag{4.4}$$

The Boltzmann distribution corresponding to the van der Waals potential (4.1) is also shown in figure 12 for the four sphere sizes. This gives the pair-distribution function for values of ξ in the range $\xi_0 < \xi < 0{\cdot}2$, and outside this range we have

$$\begin{aligned} p &= 0 \quad \text{for} \quad 0 \leqslant \xi < \xi_0 \\ &\quad 1 \quad \text{for} \quad \xi \geqslant 0{\cdot}2. \end{aligned} \tag{4.5}$$

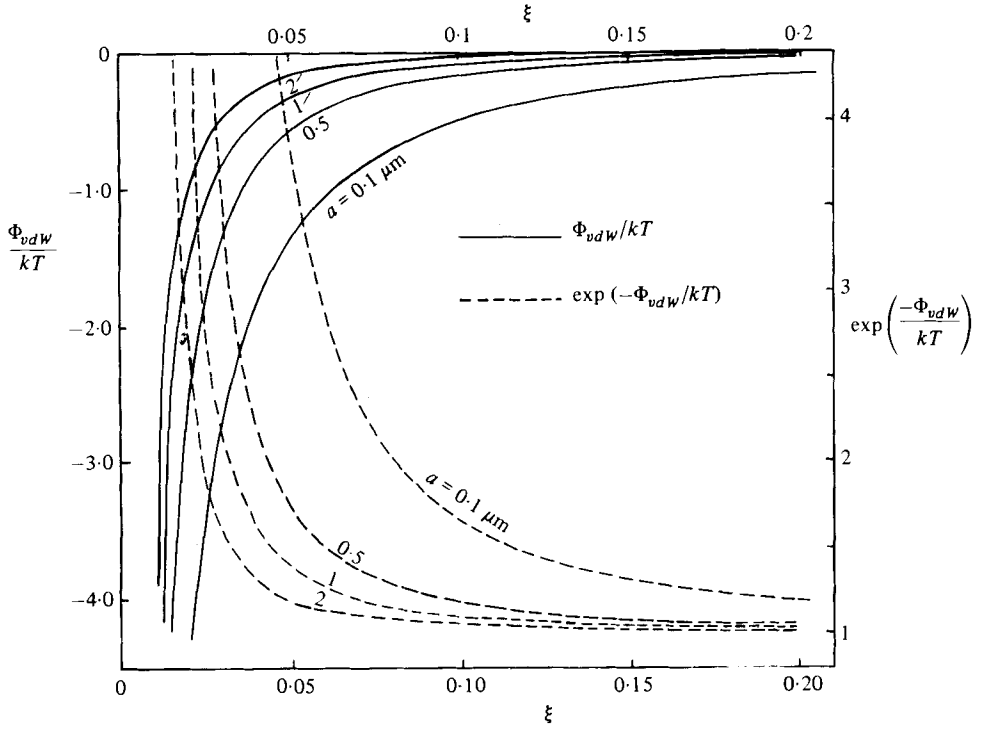

FIGURE 12. The van der Waals potential for two equal sized spheres given by (4.1), with $A/kT = 1{\cdot}25$, $\lambda_d = 0{\cdot}100\ \mu$m and various values of the radius a, as a function of the non-dimensional gap width $\xi\ (= (r-2a)/a)$. Also shown is the corresponding equilibrium pair-distribution function $\exp(-\Phi_{vdW}/kT)$.

The pair-distribution function has a very high maximum for small values of ξ_0 (ξ_0 less than about 0·02 for $a = 0{\cdot}1\ \mu$m and less than about 0·01 for $a = 1\ \mu$m), reminding us that such small values of ξ_0 are incompatible with our basic premise that the dispersion under consideration is stable.

The sedimentation coefficient S for two identical species is given by formula (6.5) in Part 1, viz.

$$S = -5 + \int_2^\infty \left\{ (A_{11} + 2B_{11} - 3 + A_{12} + 2B_{12})_{\lambda=1} \exp(-\Phi/kT) - \frac{3}{s} \right\} s^2\, ds \qquad (4.6a)$$

$$= -6{\cdot}55 + \int_2^\infty \left\{ (A_{11} + 2B_{11} - 3 + A_{12} + 2B_{12})_{\lambda=1} \left\{ \exp(-\Phi/kT) - 1 \right\} s^2\, ds. \right. \qquad (4.6b)$$

Numerical evaluation of the integral in (4.6*b*) for the interparticle potential described above is straight-forward, and the results are shown in table 4 and figure 13 in the form of S as a function of ξ_0, the location of the Coulomb potential barrier, for each of the four different sphere radii.

It was pointed out in Part 1 that since the combination of mobility functions in the integrand in (4.6*b*) is approximately equal to 1·32 over the range $2 < s < 2{\cdot}2$, an approximate form of (4.6*b*) is

$$S = -6{\cdot}55 + 0{\cdot}44\alpha, \qquad (4.7)$$

	$a = 0{\cdot}1\ \mu$m		$a = 0{\cdot}5\ \mu$m		$a = 1\ \mu$m		$a = 2\ \mu$m	
ξ_0	S	α	S	α	S	α	S	α
0·008	—	—	—	—	—	—	−5·47	2·39
0·010	—	—	—	—	−4·83	3·79	−6·12	0·96
0·012	—	—	−3·79	6·09	−5·74	1·79	−6·30	0·54
0·014	—	—	−5·08	3·26	−6·05	1·10	−6·39	0·34
0·016	−0·58	13·23	−5·60	2·11	−6·21	0·75	−6·45	0·22
0·018	−2·65	8·68	−5·87	1·51	−6·31	0·54	−6·49	0·12
0·020	−3·66	6·44	−6·03	1·15	−6·37	0·39	−6·52	0·05
0·025	−4·93	3·63	−6·27	0·63	−6·48	0·15	−6·59	−0·08
0·030	−5·44	2·49	−6·40	0·35	−6·55	−0·01	−6·63	−0·19
0·040	−5·97	1·32	−6·56	−0·01	−6·66	−0·25	−6·71	−0·37
0·050	−6·24	0·70	−6·67	−0·26	−6·74	−0·43	−6·78	−0·52
0·070	−6·58	−0·05	−6·84	−0·65	−6·89	−0·76	−6·91	−0·81
0·100	−6·91	−0·80	−7·06	−1·14	−7·08	−1·20	−7·10	−1·23
0·150	−7·34	−1·78	−7·39	−1·90	−7·40	−1·92	−7·40	−1·93
0·200	−7·71	−2·65	−7·71	−2·65	−7·71	−2·65	−7·71	−2·65

TABLE 4. Values of the sedimentation coefficient S for a dispersion of identical spheres of radius a as a function of the parameter ξ_0 specifying the location of the high Coulomb potential barrier. α is the corresponding excess fraction of close particle pairs divided by the volume fraction ϕ.

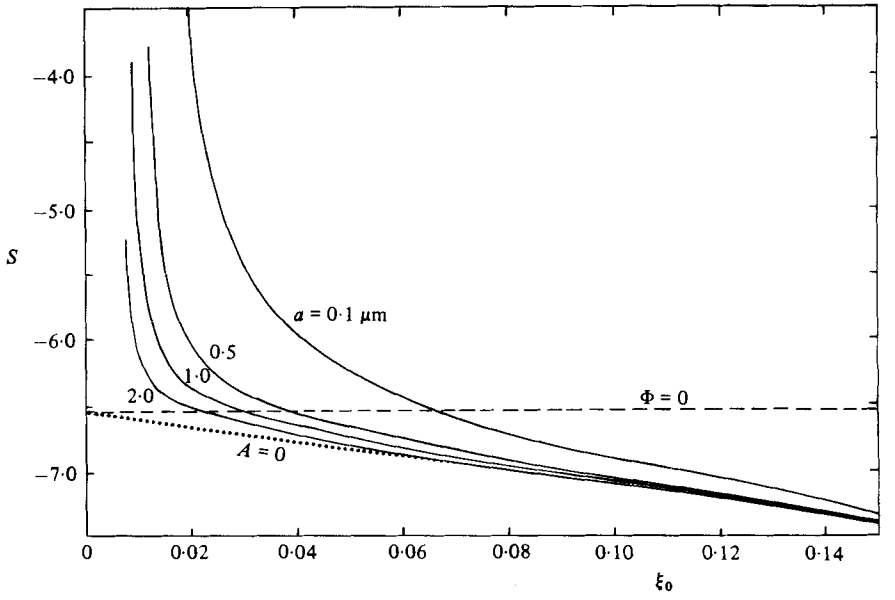

FIGURE 13. The sedimentation coefficients for a dispersion of identical spheres of radius a as a function of the parameter ξ_0 specifying the location of the high Coulomb potential barrier surrounding each sphere. The dotted curve labelled $A = 0$ corresponds to the case of zero van der Waals attraction (that is, Coulomb forces only).

where

$$\alpha = 3\int_2^\infty (e^{-\Phi/kT}-1)\,s^2\,ds = \frac{n}{\phi}\int_{r\geqslant 2}(p-1)\,d\mathbf{r}, \tag{4.8}$$

and $\alpha\phi$ can be interpreted as the excess number of spheres (excess to the number for $p = 1$) which are partners in close pairs for which $s < 2{\cdot}2$, expressed as a fraction of all the spheres. We have tested the accuracy of (4.7) by calculating α from (4.8), with results which are included in table 4. The agreement between the two expressions (4.6) and (4.7) is found to be good, the difference being less than 1 % over all parts of the table. Values of α exceeding 15 are unlikely to be compatible with stability of the dispersion, and our calculations have therefore been confined to values of ξ_0 for which $\alpha < 15$. Aside from its use as a parameter which determines the sedimentation coefficient, the value of α conveys information about the structure of the dispersion. The relation (4.7) may therefore have value for experimental purposes.

Figure 13 shows that the value of S depends quite strongly on ξ_0 at small values of ξ_0. Small values of ξ_0 imply a small double-layer thickness and a correspondingly large range of action of attractive forces and a positive excess number of close pairs ($\alpha > 0$), and since close pairs fall more quickly than well separated pairs the value of S is greater than $-6{\cdot}55$. Large values of ξ_0 on the other hand imply the exclusion of pairs over a wider range of gap thicknesses and a deficiency of close pairs ($\alpha < 0$), and the associated values of S are less than $-6{\cdot}55$. The value of ξ_0 at which $\alpha = 0$ (interparticle force effects being present still, but cancelling) depends on the sphere radius, and varies from 0·022 for $a = 2$ μm to 0·065 for $a = 0{\cdot}1$ μm.

Incidentally, we may gain some idea of the effect of a variation in the composite Hamaker constant A by comparing the above results (for $A = 5{\cdot}0\times 10^{-21}$ J) with those obtained for $A = 0$. In this latter case

$$\exp(-\Phi/kT) = 0 \quad \text{when} \quad 0 < \xi < \xi_0$$
$$1 \quad \text{when} \quad \xi \geqslant \xi_0,$$

and if we approximate to the bracketed sum of mobility functions in (4.6*b*) in the same manner as in (4.7) we find

$$S \approx -6{\cdot}55 - 5{\cdot}3(\xi_0 + \tfrac{1}{2}\xi_0^2), \tag{4.9}$$

which is shown in figure 13.

Some previous authors have investigated the effect of interparticle forces on the sedimentation coefficient for a monodisperse system, although there are few quantitative results. The first were Goldstein & Zimm (1971) who adopted a force potential which represents the van der Waals attraction and Coulomb repulsion more realistically than our model. The range of their calculations was limited to suit their purpose, viz. to obtain an expression for S in terms of the Hamaker constant A which would allow the value of A to be inferred from a previous observation of the mean particle velocity; and their expression for S differs from ours slightly in consequence of an error of principle in their calculation of the mean velocity of a particle in an ambient flow field due to the presence of a second particle. In later work which also is in error in this part of the calculation, Reed & Anderson (1976) adopted a realistic form of the Coulomb repulsion potential but ignored the van der Waals potential, and found values of S less than that for $\Phi = 0$ which they recognized as being a consequence of the greater fall speed of the excluded close pairs. Most recently, Dickinson (1980) adopted the same high discontinuous Coulomb barrier as in our model but ignored the van der Waals force, and then used far-field asymptotic forms

for the mobility functions to evaluate the integral in the expression for S, thereby obtaining an approximate version of (4.9). Dickinson makes the valid comment that the values of the mobility functions for small values of $r-2a$, which are difficult to calculate (although they are now available), become less relevant as the distance of the high potential barrier from the surface of a particle is increased. A similar comment may be made about polydisperse systems, because many of the integrals weighted with the factor $\exp(-\Phi_{ij}/kT)$ there involve also a pair-distribution function whose form near $s = 2$ is not easily found, as well as mobility functions whose values are now known.

A number of observations of the settling speed of uniform colloidal spheres in a dilute liquid suspension have been made, usually under conditions such that the double layer thickness is a small fraction of the sphere radius (corresponding to a fairly high electrolytic strength of the liquid). The observed values of the sedimentation coefficient S have generally been in the range -5 to -6. Cheng & Schachman (1955) used polystyrene latex spheres of radius 0·13 μm dispersed in a sodium chloride solution (0·098 mol dm^{-3}), and found $S = -5{\cdot}1$. More recently, Buscall *et al.* (1982) also used polystyrene latex spheres, of radius 1·55 μm, dispersed in a sodium chloride solution (10^{-3} mol dm^{-3}), and their measurements gave $S = -5{\cdot}4 \mp 0{\cdot}1$. Goldstein & Zimm (1971) estimated that in the conditions of Cheng & Schachman's experiments the double layer thickness, or Debye–Hückel screening length (κ^{-1}), was $1{\cdot}0 \times 10^{-3}$ μm, $= 0{\cdot}0077a$; and with the 100 times weaker electrolyte used in the experiments of Buscall *et al.* the double layer thickness would be 10 times larger and so equal to $0{\cdot}0065a$ for these latter experiments.

We may try to relate these measurements of S to the calculated values shown in figure 13 by choosing the value of the distance $\xi_0 a$ at which the van der Waals attraction is cut off in our simplified interparticle potential so as to make the calculated value of S agree with the measured value. According to figure 13, $S = -5{\cdot}1$ for spheres of radius 0·13 μm when $\xi_0 = 0{\cdot}020$, that is, about 2·6 times the D.–H. length in Cheng & Schachman's experiments, and $S = -5{\cdot}4$ for spheres of radius 1·55 μm when $\xi_0 = 0{\cdot}009$, that is, about 1·4 times the D.–H. length in the experiments of Buscall *et al.* These are plausible values of ξ_0, and the fact that the values of $\xi_0 \kappa a$ are above unity is understandable, because the Coulomb potential remains appreciable until the sphere gap exceeds about two double-layer thicknesses. The height of the Coulomb barrier under the experimental conditions is of course also relevant to a choice of ξ_0, but information on this is not available. It seems reasonable to conclude that the positive differences between these measured values of S and $-6{\cdot}55$ could be a consequence of van der Waals attractive forces causing an excess number of close pairs whose common speed of fall exceeds the fall speed of an isolated sphere.

Another set of measurements was made recently by Kops-Werkhoven & Fijnaut (1981) who used sterically stabilized silica spheres of radius 0·021 μm dispersed in cyclohexane, and found $S = -6 \mp 1$. This value of S corresponds to a value of ξ_0 of about 0·1 if the interparticle potential has the form assumed here. It does not seem possible to infer the position of the effective potential barrier surrounding these silica particles from the data given by Kops-Werkhoven & Fijnaut, although a value near 0·1 is plausible.

4.3. *Spheres of different density at small Péclet number*

We consider now the sedimentation coefficient for a system of spherical particles of the same size but different densities, with the Péclet number of the pair interactions

assumed to be small, as is usually the case when effects of interparticle forces are significant. The assumption of equal sphere sizes is one of expediency, to keep within bounds the complexity of what are intended to be exploratory calculations.

We shall adopt the same form of interparticle force potential as for the case of identical spheres. The composite Hamaker constant A in reality depends on the densities and molecular compositions of the two spheres and the fluid medium, but for definiteness we shall again adopt the value of A appropriate to polystyrene particles in water, viz. $5{\cdot}0\times10^{-21}$ J. The resultant potential Φ_{ij} indicated in figure 11, with numerical values of the van der Waals potential given by (4.1) and shown in figure 12, is thus again applicable and ξ_0 and a/λ_d are the only variable parameters.

The pair-distribution function at small Péclet number was shown in Part 1 to be of the form

$$p_{ij}(\mathbf{r}) = \exp\{-\Phi_{ij}(r)/kT\}\left\{1+\mathscr{P}_{ij}\frac{\mathbf{r}\,.\,\mathbf{V}_{ij}^{(0)}}{rV_{ij}^{(0)}}Q(s)\right\}$$

correct to the order of $\mathscr{P}_{ij}$, where Q satisfies the equation

$$\frac{d}{ds}\left(s^2G\frac{dQ}{ds}\right)-\frac{d(\Phi_{ij}/kT)}{ds}s^2G\frac{dQ}{ds}-2HQ = s^2W-\frac{d(\Phi_{ij}/kT)}{ds}s^2L \tag{4.10}$$

and the boundary conditions

$$Q\to0 \quad \text{as} \quad s\to\infty, \tag{4.11}$$

$$G\,dQ/ds = 0 \quad \text{at} \quad s = 2. \tag{4.12}$$

(It will be noticed incidentally, although we have not made any use of the observation, that equation (4.10) is recovered from (3.2) – the equation for $Q(s)$ when $\Phi_{ij}=0$ – if all the mobility functions making up G, H and W in the latter equation are replaced by their product with $\exp(-\Phi_{ij}/kT)$.)

With our assumed form for $\Phi_{ij}(r)$, the terms involving Φ_{ij} in (4.10) are non-zero only in the range $2+\xi_0 < s < 2{\cdot}2$, and there are discontinuities in Φ_{ij} at $s = 2+\xi_0$ and $s = 2{\cdot}2$. If we think of each of these two jumps as being made over a small range of values of s of order δ, then within this range $d\Phi_{ij}/ds$ has large magnitude and (4.10) reduces approximately to

$$dQ/ds = L/G, \tag{4.13}$$

and since L/G is finite (and equal to unity for all values of s when $\lambda = 1$) the change in Q across the transition is of order δ and so is negligible for our model potential. The jumps can therefore be ignored, and the effect on $Q(s)$ of the terms involving Φ_{ij} in the open interval $2+\xi_0 < s < 2{\cdot}2$ alone need be considered.

It seems unlikely that this effect is a large one. When $\lambda = 1$ we have

$$L\sim2\xi, \quad W\to1{\cdot}599$$

as $\xi\to0$, and so, with the van der Waals form (4.1) for Φ_{ij},

$$\frac{s^2L}{s^2W}\frac{d(\Phi_{ij}/kT)}{ds}\sim\frac{0{\cdot}12}{\xi}, \tag{4.14}$$

showing that the ratio of the new and old terms on the right-hand side of (4.10) is of order unity except when ξ is as small as 0·01 (and smaller values are irrelevant because they imply too small a value of ξ_0 for the assumed stability of the dispersion). And when ξ does have a value near 0·01, and the two terms involving Φ_{ij} in (4.10) are dominant, the equation reduces to (4.13), giving $dQ/ds = 1$, which is not very different from the value of dQ/ds at $\xi = 0$ in the absence of the interparticle force (viz. about 0·8). The modification to $Q(s)$ resulting from the presence of the terms

involving Φ_{ij} in (4.10) in a numerical integration beginning at a large value of s and proceeding towards $s = 2$ is thus equivalent to an order-one change in the derivatives of Q in the last stages of the integration ($2 < s < 2{\cdot}2$) where Q is already close to its terminal value. (See the curve for $\lambda = 1$ in figure 9, showing the calculated values of Q in the absence of the interparticle force.) Since the inner boundary condition (4.12) is independent of Φ_{ij}, it seems that the change in Q due to the presence of the interparticle force will be a minor one, except possibly at the smallest (and least realistic) values of ξ_0. Bearing in mind that, as will soon be seen, the sedimentation coefficient depends only weakly on $Q(s)$ (because the dominant contribution to S_{ij}, viz. that due directly to gravity, is independent of Q), we concluded that Q could be regarded, with sufficient accuracy for the present purposes, as independent of Φ_{ij}. The values of $Q(s)$ shown in figure 9 for $\lambda = 1$ (which is applicable for any value of γ except $\gamma = 1$) were therefore used in the present calculation of the effect of the interparticle force on S_{ij}.

The sedimentation coefficient S_{ij} is here the sum of three direct contributions, made by gravity, interparticle force, and Brownian diffusion:

$$S_{ij} = S_{ij}^{(G)} + S_{ij}^{(I)} + S_{ij}^{(B)}, \tag{4.15}$$

where $S_{ij}^{(G)}$, $S_{ij}^{(I)}$ and $S_{ij}^{(B)}$ are given by (6.10), (6.11) and (6.12) in Part 1. Moreover, in this case of a small departure from equilibrium due to gravity we may again write $Q(s)$ as in (3.5) and S_{ij} as in (3.6). Each of the three terms in (4.15) is similarly a linear function of γ, that is,

$$S_{ij}^{(G)} = S_{ij}'^{(G)} + \gamma S_{ij}''^{(G)}, \text{ etc}, \tag{4.16}$$

and the explicit expressions for $S_{ij}'^{(G)}$, etc are seen from (6.10), (6.11) and (6.12) in Part 1 to be, for the case $\lambda = 1$, as follows:

$$S_{ij}'^{(G)} = \int_2^\infty (A_{11} + 2B_{11} - 3)_{\lambda=1} \exp(-\Phi_{ij}/kT)\, s^2\, ds, \tag{4.17}$$

$$S_{ij}''^{(G)} = \int_2^\infty \left\{ (A_{12} + 2B_{12})_{\lambda=1} \exp(-\Phi_{ij}/kT) - \frac{3}{s} \right\} s^2\, ds - 5, \tag{4.18}$$

$$S_{ij}'^{(I)} = \frac{1}{2} \int_2^\infty (A_{12} - A_{11})_{\lambda=1} \frac{d \exp(-\Phi_{ij}/kT)}{ds} Q'(s)\, s^2\, ds, \tag{4.19}$$

$$S_{ij}'^{(B)} = \int_2^\infty \left(\frac{A_{11} - B_{11}}{s} + \frac{1}{2}\frac{dA_{11}}{ds} - \frac{A_{12} - B_{12}}{s} - \frac{1}{2}\frac{dA_{12}}{ds} \right)_{\lambda=1} \times \exp(-\Phi_{ij}/kT)\, Q'(s)\, s^2\, ds. \tag{4.20}$$

The expressions for $S_{ij}''^{(I)}$ and $S_{ij}''^{(B)}$ are the same as those for $S_{ij}'^{(I)}$ and $S_{ij}'^{(B)}$ with Q' replaced by Q'', and since $Q' = -Q''$ when $\lambda = 1$ we have in the present case

$$S_{ij}'^{(I)} = -S_{ij}''^{(I)} \quad \text{and} \quad S_{ij}'^{(B)} = -S_{ij}''^{(B)}. \tag{4.21}$$

Numerical evaluation of the integrals (4.17), (4.18) and (4.20) is quite straightforward. In the case of (4.19) we note that our assumed form of Φ_{ij} contains jumps at $s = 2 + \xi_0$ and $s = 2{\cdot}2$. On interpreting these jumps as limits of continuous functions

	$a = 0{\cdot}1\ \mu$m		$a = 0{\cdot}5\ \mu$m		$a = 1\ \mu$m		$a = 2\ \mu$m	
ξ_0	$S'^{(G)}_{ij}$	$S''^{(G)}_{ij}$	$S'^{(G)}_{ij}$	$S''^{(G)}_{ij}$	$S'^{(G)}_{ij}$	$S''^{(G)}_{ij}$	$S'^{(G)}_{ij}$	$S''^{(G)}_{ij}$
0·008	—	—	—	—	—	—	−2·08	−3·39
0·010	—	—	—	—	−2·22	−2·62	−1·93	−4·19
0·012	—	—	−2·45	−1·36	−2·01	−3·73	−1·88	−4·42
0·014	—	—	−2·14	−2·94	−1·93	−4·12	−1·86	−4·53
0·016	−3·09	2·49	−2·03	−3·57	−1·90	−4·31	−1·85	−4·60
0·018	−2·63	−0·04	−1·97	−3·91	−1·88	−4·43	−1·84	−4·65
0·020	−2·41	−1·27	−1·93	−4·11	−1·86	−4·51	−1·83	−4·69
0·025	−2·14	−2·81	−1·88	−4·39	−1·84	−4·65	−1·82	−4·77
0·030	−2·03	−3·44	−1·85	−4·55	−1·82	−4·73	−1·81	−4·83
0·040	−1·92	−4·05	−1·82	−4·74	−1·80	−4·86	−1·79	−4·92
0·050	−1·87	−4·38	−1·80	−4·87	−1·79	−4·96	−1·78	−5·01
0·060	−1·83	−4·60	−1·78	−4·98	−1·77	−5·05	−1·77	−5·08
0·080	−1·79	−4·92	−1·75	−5·17	−1·75	−5·21	−1·74	−5·23
0·100	−1·75	−5·16	−1·73	−5·33	−1·73	−5·36	−1·72	−5·37
0·150	−1·69	−5·65	−1·68	−5·71	−1·68	−5·72	−1·68	−5·73
0·200	−1·63	−6·08	−1·63	−6·08	−1·63	−6·08	−1·63	−6·08

TABLE 5. Values of the direct contributions to S'_{ij} and S''_{ij} (where $S_{ij} = S'_{ij} + \gamma S''_{ij}$) due to gravity as a function of ξ_0, for two species of spheres of equal radius a at small Péclet number

	$a = 0{\cdot}1\ \mu$m		$a = 0{\cdot}5\ \mu$m		$a = 1\ \mu$m		$a = 2\ \mu$m	
ξ_0	$S'^{(I)}_{ij}$	$S'^{(B)}_{ij}$	$S'^{(I)}_{ij}$	$S'^{(B)}_{ij}$	$S'^{(I)}_{ij}$	$S'^{(B)}_{ij}$	$S'^{(I)}_{ij}$	$S'^{(B)}_{ij}$
0·008	—	—	—	—	—	—	0·51	0·54
0·010	—	—	—	—	0·68	0·68	0·15	0·37
0·012	—	—	0·98	0·91	0·26	0·44	0·07	0·31
0·014	—	—	0·47	0·58	0·15	0·36	0·04	0·29
0·016	2·03	1·52	0·29	0·45	0·09	0·33	0·02	0·28
0·018	1·14	1·03	0·18	0·39	0·06	0·30	0·005	0·27
0·020	0·92	0·81	0·14	0·35	0·04	0·29	−0·004	0·26
0·025	0·39	0·53	0·06	0·31	0·002	0·26	−0·02	0·25
0·030	0·26	0·42	0·02	0·27	−0·02	0·25	−0·04	0·24
0·040	0·10	0·32	−0·03	0·24	−0·05	0·23	−0·06	0·22
0·050	0·03	0·28	−0·06	0·22	−0·07	0·22	−0·08	0·21
0·060	−0·02	0·25	−0·08	0·21	−0·09	0·20	−0·09	0·20
0·080	−0·08	0·21	−0·11	0·19	−0·12	0·18	−0·12	0·18
0·100	−0·12	0·18	−0·14	0·17	−0·14	0·17	−0·14	0·17
0·120	−0·15	0·17	−0·16	0·16	−0·16	0·16	−0·16	0·16
0·150	−0·18	0·15	−0·19	0·14	−0·19	0·14	−0·19	0·14
0·200	−0·23	0·12	−0·23	0·12	−0·23	0·12	−0·23	0·12

TABLE 6. Values of the direct contributions to S'_{ij} (where $S_{ij} = S'_{ij} + \gamma S''_{ij}$) made by the interparticle force ($S'^{(I)}_{ij}$) and by Brownian diffusion ($S'^{(B)}_{ij}$) as a function of ξ_0, for two species of spheres of equal radius a at small Péclet number. The corresponding contributions to S''_{ij} are equal in magnitude and opposite in sign to those made to S'_{ij}.

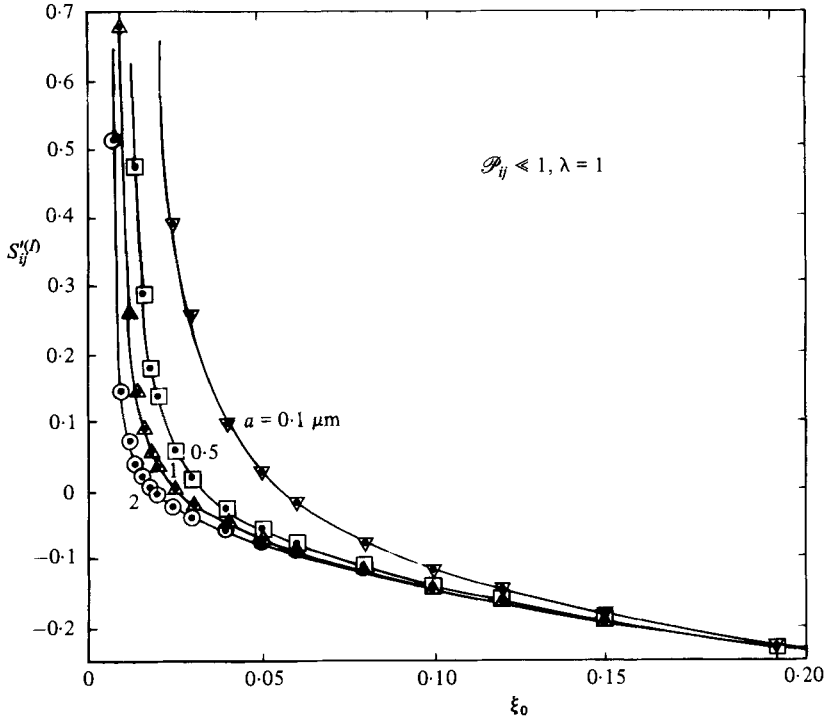

FIGURE 14. The direct contribution to S'_{ij} made by the interparticle force as a function of ξ_0 for two species of spheres of equal radius a at small Péclet number.

we find

$$S'^{(I)}_{ij} = \frac{1}{2}\lim_{s\downarrow 2+\xi_0}\left\{(A_{12}-A_{11})_{\lambda=1}\exp(-\Phi_{ij}/kT)\,Q'(s)\,s^2\right\}$$
$$+\frac{1}{2}\lim_{s\uparrow 2\cdot 2}\left\{(A_{12}-A_{11})_{\lambda=1}\{1-\exp(-\Phi_{ij}/kT)\}\,Q'(s)\,s^2\right\}$$
$$+\frac{1}{2}\int_{2+\xi_0}^{2\cdot 2}(A_{12}-A_{11})_{\lambda=1}\frac{d\exp(-\Phi_{ij}/kT)}{ds}Q'(s)\,s^2\,ds, \quad (4.22)$$

and this integral can be integrated numerically.

The calculated values of $S'^{(G)}_{ij}$ and $S''^{(G)}_{ij}$ for various values of ξ_0 and four sphere sizes are shown in table 5 and of $S'^{(I)}_{ij}$ and $S'^{(B)}_{ij}$ in table 6. The contribution to S'_{ij} of particular interest here is that made by the interparticle force. Figure 14 shows $S'^{(I)}_{ij}$ as a function of ξ_0 for the four sphere sizes. Increasing ξ_0 from its minimum value zero to its maximum value 0·2 changes the division between the range from which particles are excluded by repulsive forces and the range of attractive forces, and as would be expected $S'^{(I)}_{ij}$ changes sign at some value of ξ_0 between zero and 0·2. To account for the fact that $S'^{(I)}_{ij} > 0$ (implying that the interparticle force between a sphere of species i and a sphere of the same size but smaller density causes an increase in the speed of fall of i spheres) at smaller values of ξ_0, one must recall that $Q(s) < 0$ and that the j spheres are less numerous just above an i sphere than just below it when $\gamma < 1$, thereby causing a net downward contribution to the velocity of the i

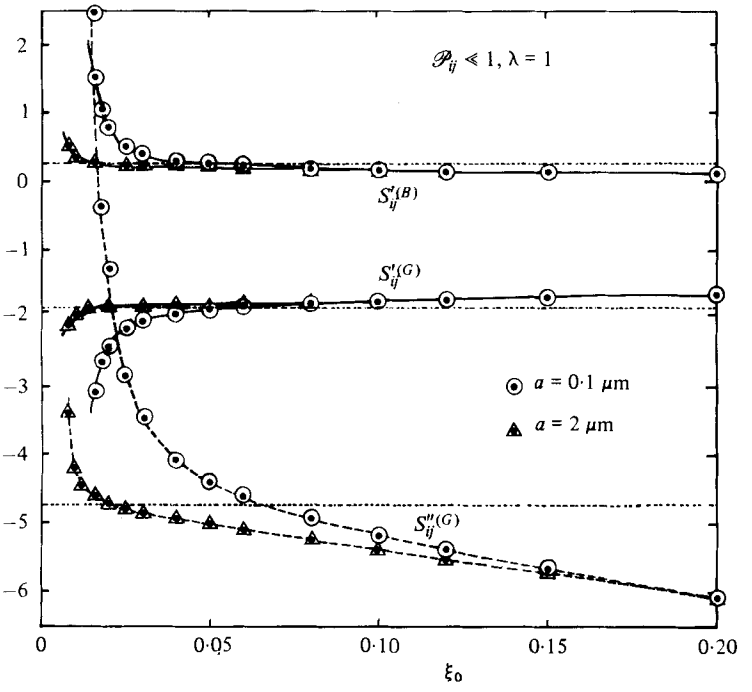

FIGURE 15. The direct contributions to S'_{ij} made by gravity and Brownian diffusion, and that made to S''_{ij} by gravity, for two species of spheres of equal radius a at small Péclet number. The three dotted straight lines show the values in the absence of interparticle forces.

sphere due to attraction by j spheres. On the other hand, at larger values of ξ_0 the Coulomb repulsion dominates and the speed of fall of the i spheres is decreased. The general magnitude of $S'^{(I)}_{ij}$ is comparable with that of $S'^{(B)}_{ij}$ in this case of equal sphere sizes, and both are significantly smaller than $|S'^{(G)}_{ij}|$ and $|S''^{(G)}_{ij}|$.

Figure 15 shows the other two contributions to S'_{ij}, for the smallest and largest of the four sphere sizes. Also shown in figure 15 is the direct contribution to S''_{ij} due to gravity. In view of (4.21) there is no need to show the contributions to S''_{ij} due to interparticle force and Brownian diffusion. From a comparison of the curves in figure 15 with the straight lines showing the values of $S'^{(G)}_{ij}$, $S'^{(B)}_{ij}$ and $S''^{(G)}_{ij}$ for the case $\Phi_{ij} = 0$, we see the importance of the indirect effect (that is, the consequence of the change in the pair-distribution function) of the interparticle force.

Finally, the three contributions are added together to show the resultant values of S'_{ij} and S''_{ij} in figure 16.

5. Discussion of results

Our numerical results are likely to be applied most often to a system of two species of particles, characterized by the suffixes i and j say. The mean velocities of the two different species are given by the general formulae

$$\left.\begin{aligned} \langle \mathbf{U}_i \rangle &= \mathbf{U}_i^{(0)}(1 + S_{ii}\,\phi_i + S_{ij}\,\phi_j) \\ \langle \mathbf{U}_j \rangle &= \mathbf{U}_j^{(0)}(1 + S_{ji}\,\phi_i + S_{jj}\,\phi_j), \end{aligned}\right\} \tag{5.1}$$

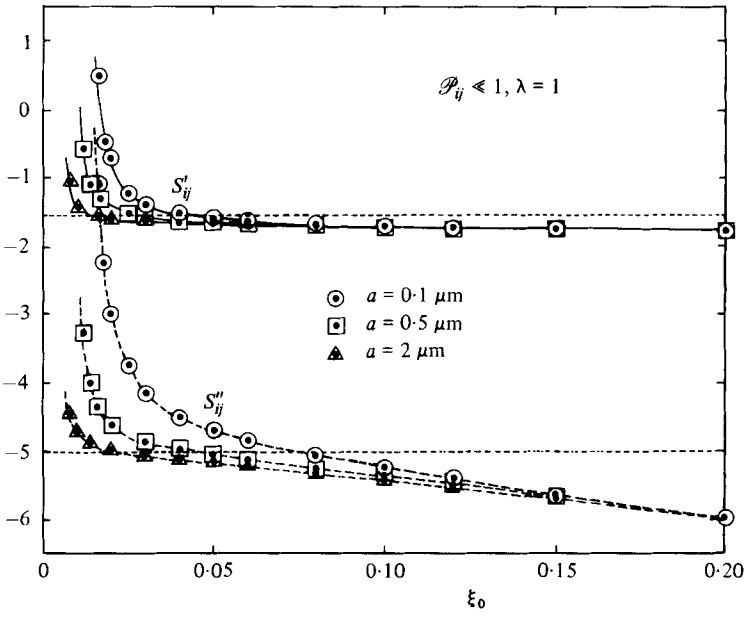

FIGURE 16. The sedimentation coefficients S'_{ij} and S''_{ij} (defined by the relation $S_{ij} = S'_{ij} + \gamma S''_{ij}$) for two species of spheres of equal radius a at small Péclet number, as functions of the parameter ξ_0 specifying the location of the high Coulomb barrier. The dotted straight lines show the values in the absence of interparticle forces.

where S_{ij} depends on $\lambda (= a_j/a_i)$ and $\gamma (= (\rho_j - \rho)/(\rho_i - \rho))$, and

$$S_{ji}(\lambda, \gamma) = S_{ij}(\lambda^{-1}, \gamma^{-1}). \tag{5.2}$$

In (5.1) S_{ii} and S_{jj} refer to interactions between identical particles. In the absence of interparticle forces $S_{ii} = S_{jj} = -6{\cdot}55$; and when interparticle forces are taken into account S_{ii} and S_{jj} may take different values, as illustrated by the calculated curves in figure 13 for a simplified form of interparticle force potential.

In some applications it will be of interest to know whether the two types of particle are sufficiently close in their properties for the formula for the sedimentation velocity in a monodisperse system to be applicable. This is not a simple question, in view of the singular character of the limit represented by identical particles. First the value of the Péclet number (defined by (1.2)) for the relative motion of the two spheres due to gravity should be calculated. If $\mathscr{P}_{ij} \ll 1$, the singular behaviour is mostly suppressed, and the calculated values of S'_{ij} and S''_{ij} in table 3 (for the case $\Phi_{ij} = 0$) allow the two sedimentation coefficients S_{ij} and S_{ji} to be estimated. If they are close to each other and to $-6{\cdot}55$, then the dispersion is effectively monodisperse. If on the other hand $\mathscr{P}_{ij} \gg 1$, S_{ij} and S_{ji} will definitely differ from $-6{\cdot}55$, by an amount which depends on whether γ or λ is closer to unity. If $|(\gamma-1)/(\lambda-1)| \ll 1$, the values of S_{ij} in table 2 are applicable and, provided $|\lambda - 1| \ll 1$, $S_{ij} \approx -5{\cdot}6$. However, if $|\lambda - 1|$ is much smaller than $|\gamma - 1|$, the relation

$$S_{ij} = -2{\cdot}52 - 0{\cdot}13\gamma$$

is applicable (see table 1). If both particles have approximately a radius of 2 μm and approximately a reduced density of 1 gm/cm^3, a size difference of four percent or a reduced density difference of eight percent would be sufficient to make the Péclet number of the relative motion equal to 10.

The magnitude of S_{ij} has been found to vary widely with γ and λ, especially for values of λ above about 2, and it may also be much greater than unity. Suppose, for example, that two species characterized by $\lambda = \frac{1}{4}$ and $\gamma = 1$ are interacting at large Péclet number and that interparticle forces are negligible. Table 1 shows that $S_{ij} = -3{\cdot}83$ and $S_{ji} = -24{\cdot}32$, whence

$$\langle \mathbf{U}_i \rangle = \mathbf{U}_i^{(0)}(1 - 6{\cdot}55\phi_i - 3{\cdot}83\phi_j)$$
$$\langle \mathbf{U}_j \rangle = \mathbf{U}_j^{(0)}(1 - 24{\cdot}32\phi_i - 6{\cdot}55\phi_j).$$

The large magnitude of S_{ji} here leads to the curious result that the sense of $\langle \mathbf{U}_j \rangle$ is reversed by the up-current caused by the falling larger i spheres if ϕ_i exceeds about 0·04. It might be thought on mathematical grounds that, since our expressions for $\langle \mathbf{U}_i \rangle$ and $\langle \mathbf{U}_j \rangle$ are perturbation expansions valid only when $\phi_i + \phi_j \ll 1$, a reversal of sign of $\langle \mathbf{U}_j \rangle$ could not occur within the range of values of ϕ_i and ϕ_j for which the expressions are valid. However, there is not necessarily a conflict. The magnitudes of our perturbation velocities $S_{ij}\phi_j \mathbf{U}_i^{(0)}$ and $S_{ji}\phi_i \mathbf{U}_j^{(0)}$ certainly must be small compared with the larger of the two imposed velocities $\mathbf{U}_i^{(0)}$ and $\mathbf{U}_j^{(0)}$, but they may be comparable with one of them if this one is much smaller than the other.

The calculations for the case of small Péclet numbers showed that the direct contribution to S_{ij} due to Brownian diffusion (denoted by $S_{ij}^{(B)}$) is generally rather small compared with the direct contribution due to gravity ($S_{ij}^{(G)}$). At large Péclet numbers $S_{ij}^{(B)} = 0$, and it is likely that $|S_{ij}^{(B)}|$ is considerably smaller than $|S_{ij}^{(G)}|$ at all values of the Péclet number. (A pity – recognizing that such a contribution exists and calculating its value made a nice theoretical problem.) However this does not mean that the effects of Brownian diffusion may be ignored in an approximate treatment; the indirect effect of Brownian diffusion exerted through its influence on the structure of the dispersion, that is, on the pair-distribution function in our case of a dilute dispersion, is significant at all except large Péclet numbers. The influence of Brownian diffusion on the pair-distribution function is strong in particular in the neighbourhood of the touching position ($s = 2$) where p_{ij} is singular in the absence of Brownian diffusion.

Our calculations of the effect of an interparticle force were based on a simplified form of the potential function representing strong Coulomb repulsion of spheres with a spacing less than ξ_0 and van der Waals attraction at larger spacings. A more realistic form of the potential which allowed for a continuous variation of the Coulomb contribution and a smoothly rounded secondary minimum would yield values of S_{ij} differing in numerical detail, but is unlikely to affect the conclusions concerning the magnitude of the direct contribution $S_{ij}^{(I)}$. We found that $S_{ij}'^{(I)}$ and $S_{ij}'^{(B)}$ are of comparable magnitude when $\mathscr{P}_{ij} \ll 1$ and $\lambda = 1$ (in which case $S_{ij}''^{(I)} = -S_{ij}'^{(I)}$ and $S_{ij}''^{(B)} = -S_{ij}'^{(B)}$), and there is no obvious reason why the relationship should be very different at other values of $\mathscr{P}_{ij}$ or of λ. The direct contributions to the sedimentation coefficient due to the interparticle force and relative diffusion both are non-zero only if the pair-distribution function is not completely isotropic, and so both vanish as $\mathscr{P}_{ij} \to \infty$. The remarks in the previous paragraph about the magnitude of $S_{ij}^{(B)}$ thus probably apply also to $S_{ij}^{(I)}$. The indirect effect of the interparticle force exerted through its influence on the pair-distribution function is undoubtedly important, however. We saw this clearly in the calculations of the effect of our simplified interparticle force on the sedimentation coefficient for a monodisperse system (figure 13), and similarly in the calculations of $S_{ij}^{(G)}$ for equal sized spheres at small Péclet number (figure 15). It is probable that the effect of the interparticle force would be

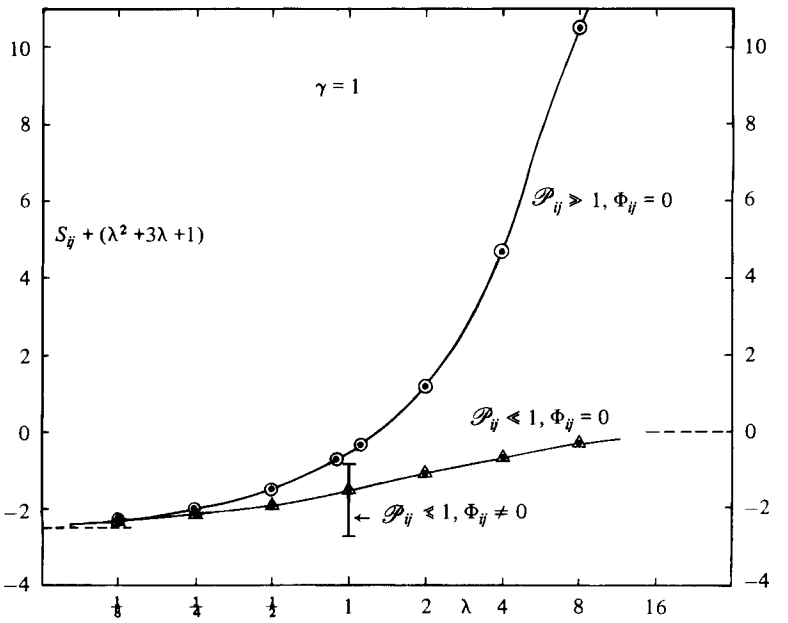

FIGURE 17. $S_{ij} + (\lambda^2 + 3\lambda + 1)$ as a function of λ for spheres of equal density ($\gamma = 1$), at small and large Péclet numbers. Both curves should asymptote to the values $-2{\cdot}5$ (as $\lambda \to 0$) and zero (as $\lambda \to \infty$), but calculations for larger values of λ are needed to confirm this in the case $\mathscr{P}_{ij} \gg 1$. For values of λ very near $\lambda = 1$, $\mathscr{P}_{ij}$ is necessarily small. The vertical line at $\lambda = 1$ shows the range of variation of $S_{ij} + (\lambda^2 + 3\lambda + 1)$ found for identical spheres of radius 1 μm as the interparticle force parameter ξ_0 varies from 0·01 to 0·20.

even more marked at large Péclet number where there would be a clash of strong processes at work in the neighbourhood of the touching position of the two spheres. The lack of any calculations of the sedimentation coefficient for two species of spheres exerting forces on each other at large Péclet number is a weakness of the existing body of information concerning polydisperse systems.

The asymptotic forms for S_{ij} at small and at large values of λ for a given (and arbitrary) value of the Péclet number put forward in Part 1 are important, because they help to set limits to the variation of S_{ij} with λ, γ and $\mathscr{P}_{ij}$ which may occur. As $\lambda \to 0$ we have

$$S_{ij} \sim -2{\cdot}5 - \gamma, \tag{5.3}$$

and the approach to this asymptotic form was found to be quite rapid, being nearly complete at $\lambda = \frac{1}{8}$ at both small and large Péclet numbers. The theoretical result for the limit $\lambda \to \infty$ is

$$S_{ij} \sim -\gamma(\lambda^2 + 3\lambda + 1). \tag{5.4}$$

The approach to this much more precise asymptotic form is slower, especially at large Péclet number, and our numerical calculations have not been taken to sufficiently large values of λ to confirm the terms of order λ and of order λ^0 in (5.4). However there is some numerical evidence to suggest that the difference between S_{ij} and the asymptotic form (5.4) diminishes when λ is above about 16. This difference is in any event a small fraction of $|S_{ij}|$ for values of λ above 2 at both small and large values of the Péclet number.

These asymptotic forms impose such strong constraints on the values of S_{ij} at small

Péclet number, where we have the additional exact information that S_{ij} is a linear function of γ, that the simple empirical relation

$$S_{ij} = \frac{-2{\cdot}5}{1+0{\cdot}6\lambda} - \gamma(\lambda^2+3\lambda+1) \tag{5.5}$$

is accurate to the first decimal place over almost the whole of the (γ,λ)-plane when $\mathscr{P}_{ij} \ll 1$. At large Péclet numbers the dependence of S_{ij} on γ and λ appears to be too complicated to allow approximate representation by simple algebraic expressions, in part owing to the strange differences of shape and position of the curves representing S_{ij} as functions of γ or λ on the two sides of the excluded ranges of these variables. There is also the difficulty of the many-valuedness of S_{ij} which occurs at the central point $\gamma = 1, \lambda = 1$. The case of spheres of equal density ($\gamma = 1$) is perhaps of greatest practical interest, and the results for this case at both small and large values of the Péclet number are shown in figure 17 in the form of $S_{ij}+(\lambda^2+3\lambda+1)$ as a function of λ. The curve for $\mathscr{P}_{ij} \gg 1$ lies above that for $\mathscr{P}_{ij} \ll 1$ because close sphere pairs, which have a larger speed of fall, are more numerous at large Péclet number. The difference between the values of S_{ij} on the two curves is rather small, except at values of λ above unity where the difference is a small fraction of $|S_{ij}|$ in any event. In the absence of evidence to the contrary, it would be reasonable to expect that S_{ij} varies monotonically with $\mathscr{P}_{ij}$ for given λ when $\Phi_{ij} = 0$.

For comparison with this range of variation of S_{ij} with Péclet number we also show on figure 17 the range of variation resulting from change of the position of the Coulomb potential barrier from $\xi_0 = 0{\cdot}02$ to $\xi_0 = 0{\cdot}20$ in the case of identical spheres of radius 1 μm which exert a force on each other.

We end by offering some conclusions relevant to further work on the problem:

(i) a rough approximation to S_{ij} in all circumstances may be obtained by retaining only the direct contribution due to gravity and ignoring those due to interparticle forces and relative diffusion;

(ii) the pair-distribution function that is substituted in the expression for $S_{ij}^{(G)}$ should in general be calculated with allowance for the effects of interparticle forces and relative diffusion;

(iii) the calculations of p_{ij} presented here are adequate for cases of negligible interparticle force effects but should be extended to other and more realistic forms of the interparticle force potential, to the case $\lambda \neq 1$ with $\Phi_{ij} \neq 0$, and, if possible, to the case of large Péclet number with $\Phi_{ij} \neq 0$;

(iv) the simple representation of the pair-distribution function in terms of the excess number of sphere pairs in the nearly-touching position that was tested and found to give accurate results for a monodisperse system in §4 provides a possible link with observations and could perhaps be exploited in other circumstances;

(v) observers of sedimentation velocities in monodisperse or polydisperse systems should take care to record the information needed for determination of the interparticle force potential under the conditions of the experiment, the range of action of strong repulsive forces being of particular importance.

We are grateful to Dr D. J. Jeffrey for putting at our disposal his numerical results and computer programmes for the two-sphere mobility functions, and for adapting his calculations to suit our needs. One of the authors (C.-S. W.) wishes to thank the Chinese Academy of Sciences, The Royal Socicty, and Trinity College for their generous support of his period of work at Cambridge.

REFERENCES

BATCHELOR, G. K. 1982 *J. Fluid Mech.* **119**, 379–408.

BUSCALL, R., GOODWIN, J. W., OTTEWILL, R. H. & TADROS, T. F. 1982 *J. Colloid Interface Sci.* **85**, 78–86.

CHENG, P. Y. & SCHACHMAN, H. K. 1955 *J. Polymer Sci.* **16**, 19.

DICKINSON, E. 1980 *J. Colloid Interface Sci.* **73**, 578–581.

FEUILLEBOIS, F. 1980 Doctoral dissertation presented to Paris VI University.

GOLDSTEIN, B. & ZIMM, B. H. 1971 *J. Chem. Phys.* **54**, 4408–4413.

JEFFREY, D. J. 1983 *J. Fluid Mech.* (submitted).

KOPS-WERKHOVEN, M. M. & FIJNAUT, H. M. 1981 *J. Chem. Phys.* **74** (3), 1618–1625.

LIN, C. J., LEE, K. J. & SATHER, N. S. 1970 *J. Fluid Mech.* **43**, 35–47.

REED, C. C. & ANDERSON, J. L. 1976 Article in *Colloid and Interface Science*, vol. IV (ed. M. Kerker). Academic Press.

SCHENKEL, J. H. & KITCHENER, J. A. 1960 *Trans. Faraday Soc.* **56**, 161.

WACHOLDER, E. & SATHER, N. S. 1974 *J. Fluid Mech.* **65**, 417–437.